JPET Fast Forward. Published on February 18, 2016 as DOI: 10.1124/jpet.115.230359
This article has not been copyedited and formatted. The final version may differ from this version.

Notoginsenoside R1 protects against neonatal cerebral hypoxic-ischemic injury through estrogen receptor-dependent activation of endoplasmic reticulum stress pathways

Yan Wang, Liu Tu, Yingbo Li, Di Chen, Shali Wang*

Cerebrovascular Diseases Laboratory, Institute of Neuroscience, Chongqing Medical University, Chongqing, China (Y.W., L.T., Y.L., D.C., S.W.)

Running Title Page

Running Title: Notoginsenoside R1 target ER stress to suppresses neonatal HIE

Corresponding Authors: Shali Wang,
Address: No.1, Yixueyuan Road, Yuzhong District, Chongqing 400016, China
Phone: +86-023-68068920;
Fax: +86-023-68892728
Email: 63557408 @qq.com

Text pages: 39
Tables: 0
Figures: 12
References: 66
Abstract: 250
Introduction: 706
Discussion: 1421

List of Abbreviations

BCL-2, B-cell lymphoma-2

CCL, common carotid artery;

CHOP, mRNA expressions of C/EBP homologous protein

ER stress, endoplasmic reticulum stress;

Ero1-α, Endoplasmic reticulum oxidoreductin-α

ERα, estrogen receptor α

ERβ, estrogen receptor β

GRP78, glucose regulated protein 78

HE, hematoxylin-eosin

HIE, hypoxic ischemic encephalopathy ;

IRE1, inositol-requiring enzyme-1;

LDH, lactate dehydrogenase;

MTT, 3-(4,5-dimethylthiazol-2-yl)-2,5-diphenyltetrazolium bromide

NeuN, neuronal nuclear antigen

NGR1, notoginsenoside R1;

OGD/R, Oxygen glucose deprivation/re-oxygenation;

PERK, double stranded RNA-activated protein kinase-like endoplasmic reticulum kinase;

SD, Sprague Dawley

TTC, 2, 3, 5, -triphenyl tetrazolium chloride

UPR, unfolded protein response;

Recommended Section

Neuropharmacology

Abstract

Notoginsenoside R1 (NGR1) is a phytoestrogen, which isolated from *Panax notoginseng*. It is used to treat many diseases including hypoxic-ischemic encephalopathy (HIE) in China, and it has been shown to target estrogen receptors. Endoplasmic reticulum (ER) stress plays an important role in the development of cell apoptosis during ischemia, and ER stress is known to be regulated by estrogen. However, neuroprotective mechanisms of NGR1 in neonatal HIE is unclear. In this study oxygen-glucose deprivation/reoxygenation (OGD/R) in primary cortical neurons and unilateral ligation of common carotid artery (CCL) followed by exposure to hypoxic environment in 7-day-old postnatal SD rats were used to mimic HIE episode. Potential neuroprotective effects of NGR1 against neonatal HIE and its mechanisms were examined. Following HIE conditions *in vitro* and *in vivo*, we administered NGR1 or the estrogen receptor inhibitor ICI-182780 and measured cell apoptosis, brain injury by MTT assay, TTC stain, et al.. Expression of estrogen receptors α (ERα) and β (ERβ), ER stress-associated proteins was detected by western blot upon stimulation with HIE, NGR1 or ICI-182780. Results showed that following HIE, ER chaperon GRP78 was activated, ER stress-associated pro-apoptotic proteins (CHOP, PERK, ERO1-α, and IRE1α) were increased, caspase-12 was increased and BCL-2 was decreased. The ER stress response and neuronal apoptosis were attenuated by NGR1 treatment. However, neuroprotective properties of NGR1 against HIE-induced apoptosis and ER stress were attenuated by ICI-182780. These results suggest that NGR1 may be an effective treatment for HIE by reducing ER stress-induced neuronal apoptosis and brain injury via estrogen receptors.

Introduction

Birth asphyxia and hypoxic-ischemic encephalopathy (HIE) remain major causes of neonatal mortality or permanent neurological morbidity in newborns. Pathological characteristics include degeneration and necrosis of nerve cells, inflammation, edema, and congestion (Northington et al., 2011; Mirza et al., 2015). Nowadays, there are no effective therapies to prevent or minimize brain damage associated with HIE injury to the perinatal brain. Some therapies have been developed for adults. However, implementation of these therapies on newborns has not been successful because pathological changes in the brain are age-dependent (Jayakara Shetty, 2015; Zhu et al., 2004). Therefore, additional treatments that are safe for children and can improve the prognosis of severe neonatal HIE are urgently needed.

Cerebral ischemia reperfusion accompanied by cell injury and apoptosis, which are believed to have necrotic features. In oxygen glucose deprivation/reoxygenation (OGD/R)-treated cortical cultures, at least 50% of dying cells show morphological characteristics of apoptosis (Badiola et al., 2011). Therefore, targeting cell apoptosis after HIE may be a promising therapeutic strategy. Endoplasmic reticulum (ER) stress is a cellular signaling response which induced by various stimuli such as oxidative stress, hypoxia-ischemia (Jiabin Guo et al., 2012), and it may cause apoptosis (Rao et al., 2004). Current studies suggest that hypoxia-ischemia causes ER stress in cells, leading to accumulation of unfolded proteins in the endoplasmic reticulum and cell apoptosis (Poone et al., 2105). Hypoxia-ischemia can activate ER stress in transient focal or global cerebral ischemia and in primary neuronal cultures following *in vitro* ischemia (Hayashi et al., 2005; Chen et al., 2008). Some studies showed that estrogen receptors regulate ER stress through CaMKII and MAPK pathway in cases of HIE (Raval et al., 2006). Adaptation to stress and establishment of ER homeostasis is achieved by activation of unfolded protein response (UPR). Increased expression of glucose regulated protein 78 (GRP78) indicates activation of the UPR and the UPR-related apoptotic process (Wu et al., 2014). Activation of ER stress results in activation of double-stranded

JPET Fast Forward. Published on February 18, 2016 as DOI: 10.1124/jpet.115.230359
This article has not been copyedited and formatted. The final version may differ from this version.

RNA-activated protein kinase-like endoplasmic reticulum kinase (PERK), inositol requiring enzyme-1 (IRE1) and activating transcription factor 6 (ATF6) (Hammadi et al., 2013). Activation of PERK and IRE1 leads to cell apoptosis, activation of ATF6 promotes cell survival (Doroudgar et al., 2013). PERK is activated by phosphorylation and triggers expression of C/EBP homologous protein (CHOP). Phospho-PERK also activates endoplasmic reticulum oxidoreductin (ERO1) that regulates Ca^{2+} in the endoplasmic reticulum and stimulates the mitochondrial apoptosis pathway (Li et al., 2009). Caspase-12 apoptosis pathways are also activated (Lakshmanan et al., 2011). IRE1 can be activated by phosphorylation, and phospho-IRE1 can inhibit the B-cell lymphoma-2 (BCL-2) pathway to promote further cell apoptosis (Xu et al., 2005).

NGR1 is a phytoestrogen, which has been used in treatment of cardiac dysfunction (Sun et al., 2013), diabetic kidney disease (Gui et al., 2014), and acute liver failure (Zhao et al., 2014). NGR1 can regulate Akt/Nrf2 pathways or TNF-α via estrogen receptor under the pathological circumstance (Lei et al.,2015; Meng et al., 2014). Li and Liu (Li et al., 2105; Liu et al., 2015) found that NGR1 could protect from renal injury via inhibition of ER stress. Results of some studies have shown that NGR1 provided neuroprotection in an adult rat model of cerebral ischemia/reperfusion via regulation of Akt/Nrf2 pathways or LC3 and Beclin 1 (Meng et al., 2104; Lu et al., 2011). NGR1 and its derivative were widely used in China for treating cerebral ischemic (Sun et al., 2011), myocardial ischemic diseases (Han et al., 1996), angina pectoris (Qin et al., 2000) and hyperlipemia (Zhang et al., 2001). However, because of the uniqueness of the neonatal brain (Hansen et al., 2004), as far as we were aware, there was no studies have examined the effects of NGR1 on HIE in neonates. It is unknown whether NGR1 can protect the neonatal brain from injury by altering cell apoptosis. Furthermore, whether NGR1 attenuates ER stress and whether NGR1 functions through estrogen receptors in cases of HIE in newborns must be assessed.

In present study, we investigated the potential neuronal protective effects of NGR1 in newborns using two models of hypoxic-ischemic injury, OGD/R of primary cortical neuron cultures and unilateral ligation of the

common carotid artery (CCL) followed by exposure to an hypoxic environment in 7-day-old rats. We also elucidated possible mechanisms that underlie NGR1 neuroprotection.

2. Methods

2.1 Drug preparation

NGR1 (chemical structure $C_{47}H_{80}O_{18}$, molecular weight = 933.13, purity>98%) was purchased from Sigma-Aldrich (Sigma-Aldrich, St. Louis, MO, USA) (Fig. 1).

2.2 Animals

Seven-day-old Sprague Dawley (SD) rats and rat fetuses were provided by the Animal Department of Chongqing Medical University (Chongqing, China). All experiments were performed in compliance with the National Institutes of Health Guide for the Care and Use of Laboratory Animals. The protocol was approved by the Animal Ethics Committee of Chongqing Medical University. All efforts were made to minimize animal suffering and the number of animals used.

2.3 Cell culture and drug treatment

Primary cortical neuron cultures were prepared from the cerebral cortices of rat fetuses (embryonic day 18) according to previously described methods (Sun et al., 2003). Cerebral cortices were removed and incubated in Ca^{2+}- and Mg^{2+}-free HBSS. The tissues were then mechanically dissociated and digested in 0.25% trypsin (with 0.02% EDTA) for 7 min at 37 °C. Trypsinization was terminated by adding DMEM supplemented with 10% FBS and the digests were centrifuged for 5 min at 1000 × *g*. Cells were then resuspended in Neurobasal Medium (Gibco, Gaithersburg, MD, USA) with 2% B-27 supplement (Gibco) and 2 mmol/L L-glutamine (Invitrogen, Gaithersburg, MD, USA). Cells were subcultured in 96-well plates (5×10^4 cells/well) for 3-(4,5-dimethyl-2-thiazolyl)-2,5-diphenyl-2H-tetrazolium bromide (MTT) assays, in 24-well plates (1×10^5 cells/well) for lactate dehydrogenase (LDH) determination and Hoechst stain, or in 6-well plates (1×10^6 cells/well) for other experiments. Plates were precoated with polyethylenimine (0.05 mg/mL, Sigma-Aldrich) overnight at 37 °C. Cultures were maintained in a Heraeus CO_2 incubator (Thermo Fisher Scientific, Rockford, IL, USA)

containing 5% CO_2, 95% air at 37 °C. Cultures were used for experiments on day 5 *in vitro*. NGR1 and ICI-182780 was dissolved in DMSO to make a stock solution (100 mmol/L) and added directly to the media. Cells were administered with NGR1 (0, 0.5, 1, 2, 5, 10, 20 μmol/L) when exposed to oxygen glucose deprivation and re-oxygenate for MTT and LDH assay. The optimal concentration of NGR1 will be selected for further experiments. In specified experiments, cells were pretreated with ICI-182780 (0.1 μmol/L) (Tocris, London, UK) (Meng et al., 2104) 2 h before OGD. DMSO (1 %) was used as vehicle.

2.4 Oxygen glucose deprivation/reoxygenation

OGD/R was performed using primary cortical neuron cultures to mimic cerebral ischemic/reperfusion injury. Experiments were conducted on day 5 of cell culture. OGD/R was performed using a modification of a previously described procedure (Chi et al., 2014). Cells were washed once with phosphate buffered saline (PBS) and culture plates were refilled with glucose-free DMEM medium. Cultures were then subjected to OGD in an anaerobic chamber (Thermo Fisher Scientific) by incubating in an anaerobic gas mixture (1% O_2, 5% CO_2, and 94% N_2) at 37 °C. After 1.5 h, cultures were removed from the anaerobic chamber, and the glucose-free Neurobasal medium was replaced with Neurobasal Medium. Cultures were then returned to a normoxic environment and were allowed to reoxygenate for 4 h to 24 h.

2.5 Hypoxia-ischemia model

HIE was mimicked by unilateral ligation of the common carotid artery (CCL) in 7-day-old SD rats followed by exposure to a hypoxic environment. Pups were anesthetized with isoflurane (2.5%) and a vertical incision was made on the neck. The right common carotid artery was located, separated from surrounding tissue, and permanently ligated. Pups were returned to a heating pad for 1 h for recovery. HIE animals were placed in an airtight chamber containing 7% humidified oxygen and 93% N_2 for 150 minutes, and a heating pad was used to maintain temperature at 35–39°C. Sham animals underwent an incision but without CCL, and the pups were

placed in a similar container but exposed to normal room air. After 150 minutes, all pups were returned to their mothers. NGR1 (0, 5, 10, 15 mg/kg•12 h) was administered to the pups by intraperitoneal injection after CLL immediately, before they exposure to the hypoxic environment. ICI-182780 (2 mg/kg) was administered to pups 2 h before CLL treatment by intraperitoneal injection (Bing Sun et al., 2013; Davis et al., 2008). Through the result of TTC stain, the optimal concentration of NGR1 will be selected and used for further experiments.

2.6 Cell viability assessment

Cell viability was determined using the MTT assay. Four or 24 h after the OGD/R challenge, cells were incubated with MTT (0.05 mg/L) for 4 h at 37 °C. The culture medium was then completely removed, and 100 μL dimethyl sulfoxide (DMSO) was added to each well to dissolve the formazan crystals. Absorbance was measured at 570 nm using a microplate reader (BIO-RAD Model 680, BIO-RAD, Hercules, California, USA). Cell viability (%) was expressed as percentage of mean experimental absorbance/mean control absorbance.

2.7 Measurement of cell membrane integrity

The rate of LDH release was used to measure membrane integrity of cells. Supernatant was collected from all cells and LDH content was determined using LDH assay kit according to the manufacturer's instructions (Nanjing Institute of Jiancheng Biological Engineering, Nanjing, China) (Mo et al., 2013). One group of cells was lysed using 0.25% Triton X-100 and the supernatant of this group was used as a positive control. The level of LDH release (%) was expressed as percentage of experimental LDH activity/positive control LDH activity.

2.8 Hoechst 33342 stain

Primary cortical neurons seeded in 24-well plates were fixed with 4% paraformaldehyde for 30 min at room temperature, washed with PBS, and stained with Hoechst 33342 (Beyotime Institute of Biotechnology, Jiangsu, China) at 37 °C for 30 min in the dark. Cells were observed under a fluorescence microscope (Olympus, Tokyo, Japan) equipped with a UV filter. Images were cached by computer. The Hoechst reagent stained the nuclei of the

cells, and apoptotic cells exhibited a bright blue fluorescence. Abnormal nuclear cells were counted between the treatment group and control group.

2.9 Evaluation of infarction volume

Cerebral infarction volume was determined by 2,3,5,-triphenyl tetrazolium chloride (TTC) (Sigma-Aldrich, MO, USA) staining. Pups were anesthetized by chloral hydrate (10%) overdose, and the brains were harvested and frozen at -20 ℃ for 10 min. The brains were then sliced into consecutive 2 mm coronal sections in a rodent brain matrix (ASI Instruments, MI, USA) and the sections were incubated in 2% TTC solution at 37 ℃ for 25 min in the dark, followed by a 24 h immersion in a 4% formaldehyde solution. The area dyed gray was defined as the infarction area. Infarction volumes were calculated with ImageJ software (NIH Image, Version 1.61, Bethesda, MD, USA) as previously described (Wang et al., 2014). To avoid the effect of edema on infarction area, we calculate the relative infarction areas of each brain section. Relative infarction area was unaffected hemisphere area minus normal hemisphere area in affected side. Infarction areas of each brain section were summed to derive total infarction areas and infarction volume was obtained by multiplying total infarction area by the thickness of the sections. The degree of cerebral infarction was presented as the percentage of infarction volume to total brain volume.

2.10 Hematoxylin-eosin staining

Hematoxylin-eosin (HE) staining was performed on paraffin sections of ischemic brain tissue. Anesthetized rats were perfused with saline followed by 4% paraformaldehyde solution. The brains were then harvested and immersed in 4% paraformaldehyde for more than 24 h. After dehydrating and vitrifying, the brains were embedded in paraffin and cut into 4 μm sections. Sections were adhered to glass slides precoated with polyethylenimine (0.01%, Sigma-Aldrich). Paraffin-embedded brain sections were dewaxed with xylene, rehydrated through an ethanol series (absolute, 95%, 90%, 80%, and 70%) and washed with water. Sections were then stained with HE

and images were collected under a microscope.

2.11 Western blots

Western blot analysis was used to quantify protein expression. Cells and brain tissues were placed in lysis buffer (Beyotime Institute of Biotechnology) and the lysate was cleared by centrifugation at 12,500 rpm for 15 min. Protein concentration was measured by a BCA protein assay kit (Thermo Fisher Scientific). Protein samples were mixed with sodium dodecyl sulfate gel-loading buffer and heated for 5 min at 100 °C, Samples were then separated by electrophoresis using a sodium dodecyl sulfate polyacrylamide gel and transferred to a PVDF membrane. Membranes were blocked for 2 h at room temperature in nonfat dry milk in TBST (10 mmol/L Tris, 150 mmol/L NaCl, pH 7.6, plus 0.1 % Tween-20). Next, membranes were incubated with primary antibody at 4 °C overnight. After washing with TBST, membranes were incubated in secondary antibody for 2 h at room temperature. Bands were scanned and densitometrically analyzed by automated ImageJ software (NIH Image, Version 1.61). Band densities for indicated phosphoproteins were normalized to corresponding band densities for total protein signals, and the indicated total proteins were expressed relative to β-actin signals.

2.12 Immunofluorescence

Immunofluorescence of brain tissue was performed on paraffin sections, which were prepared using the same method as in HE staining. After dewaxing and rehydrating, antigen was retrieved by immersing sections in citric acid buffer (pH 6.0) and heating in a microwave. This was followed by incubation in 10% normal goat serum for 120 min at room temperature. Sections were then incubated with primary antibodies: anti-GRP78 (1:50, Cell Signaling Technology, Boston, MA, USA) and anti-neuronal nuclear antigen (NeuN) (1:50, Abcam, Cambridge, UK) overnight at 4 °C in 0.01 M PBS. Next, sections were washed with PBS for 30 min and incubated for 50 min at 37 °C with Alexa Fluor 488-labeled goat anti-mouse IgG (1:100, Beyotime Institute of Biotechnology) and Alexa Fluor 555-labeled goat anti-rabbit IgG (1:100, Beyotime Institute of Biotechnology) at room temperature.

Sections were incubated in DAPI (Sigma-Aldrich) for 2 min to counterstain nuclei. Finally, sections were washed with PBS and each section image was captured with fluorescence microscope (Olympus).

2.13 Terminal-deoxynucleoitidyl transferase mediated nick end labeling (TUNEL) and Neuron-specific nuclear protein staining

Histological examination of ischemic brain paraffin sections was performed using Neuron-specific nuclear protein (NeuN) and Terminal-deoxynucleoitidyl transferase mediated nick end labeling (TUNEL) staining. Sections were dewaxed by xylene and rehydrated using a series of ethanols (absolute, 95%, 90%, 80%, 70%, diluted in double-distilled water). After incubation with anti-NeuN (1:50, Abcam) and Alexa Fluor 555-labeled goat anti-mouse IgG (1:100, Beyotime Institute of Biotechnology), the TUNEL reaction mixture (Thermo Fisher Scientific) was added and samples were incubated for 60 min at 37℃ in a humidified atmosphere in the dark. This was followed by incubation in DAPI for 2 minutes. Samples were examined under a fluorescence microscope (Olympus) using an excitation wavelength of 450-500 nm (green) and a detection wavelength of 515-565 nm (red). The proportion of TUNEL positive cells nuclei were counted between the number of TUNEL positive nuclei and number of total nuclei.

2.14 Statistical analysis

All data are expressed as mean + standard deviation (SD). Statistical analyses were performed by SPSS version 17.0 (SPSS, Chicago, IL, USA). One-way analysis of variance (ANOVA) was used to determine the significance of differences among experimental groups. A *p*-value of 0.05 was regarded as the level of statistical significance.

3. Results

3.1 NGR1 decreases vulnerability of neurons to OGD/R

Apoptosis and injury of primary cortical neurons were detected by MTT assay, measurement of LDH release, and Hoechst 33342 stain at 4 h and 24 h after OGD/R. Results showed that NGR1 (0.5, 1, 2, 5, 10, 20 μmol/L) μmol/L) did not affect normal cell growth, cell viability (Fig. 2A, B), and LDH release (Fig. 2C, D), which did not differ from the sham-OGD group. OGD/R significantly decreased cell viability (Fig. 3A, B) and clearly increased release of LDH (Fig. 3C, D) in primary cultures of cortical neurons. Treatment with NGR1 significantly attenuated cell apoptosis compared with the untreated OGD-induced primary cortical neurons (Fig. 3). The protective effect of NGR1 was evident 4 h after OGD/R at a dose as low as 10 μmol/L, and the effect was dose-dependent. At 24 h after OGD/R, 5 μmol/L NGR1 showed a treatment effect, but 10 μmol/L was the optimal dose. Results showed that NGR1 provided neuroprotective effects at concentrations of 10 μmol/L and 20 μmol/L. Therefore, we selected 10 μmol/L and a 24 h treatment period for further experiments.

To characterize OGD-induced cell death in primary cortical neurons, morphological changes of nuclei were examined by Hoechst 33342 staining (Fig. 3E, F). After treatment with OGD/R for 4 h or 24 h, apoptotic morphological changes were observed. In the control group, nuclei were round and homogeneously stained, but OGD/R-treated cells showed granular apoptotic bodies, and nuclei were pyknotic or fragmented. In the NGR1 (10 μmol/L) group, fewer granular apoptotic bodies were observed and nuclei were similar to those in the control group.

3.2 NGR1 attenuated HIE-induced brain injury in newborn rats

To quantify the infarction, brain slices were examined using TTC staining and planimetry. Images of 5 slices from each brain were analyzed using ImageJ software (NIH Image, Version 1.61). Brain damage was expressed as the ratio of total infarction volume (white area in the left side) to total brain volume. As shown in Fig. 4B, 41% of

brain slices in the HIE group were not stained (white area) which indicated infarction areas, while NGR1 (15 mg/kg•12 h) treatment remarkably reduced infarction volume (Fig. 4B). The results showed that NGR1 obviously decreased HIE-induced infarction volume. The concentration of 15 mg/kg•12 h was selected for further experiments.

Examination of the HIE *in vivo* model with HE staining revealed that 24 h after HIE, hyperaemia, cellular edema and tissue raritas were evident in the HIE group. As shown in Fig. 4C, in the NGR1 (15 mg/kg•12 h) group, there was less tissue damage, and there were more neurons and fewer cellular edema in the cerebral cortex.

As shown in Fig. 4D,E, photomicrographs showed that HIE induced significant injury of cerebral cortical neurons, as indicated by a marked increase in the number of TUNEL-positive cells compared with the sham HIE group. Intriguingly, NGR1 (15 mg/kg•12 h) treatment strongly attenuated neuron cell death as evidenced by a decreased number of TUNEL-positive cells and an increased number of NeuN-positive cells compared with the HIE group.

3.3 Increase in ER Stress during hypoxia-ischemia

Western blot analysis was used to detect expression levels of GRP78 at different times of reperfusion in primary cortical neuron cells and the brain. GRP78 is a central regulator of endoplasmic reticulum homeostasis, playing multiple roles in protein folding and activation of transmembrane endoplasmic reticulum sensors. As shown in Fig. 5A, western blot analysis revealed that in cortical neurons, GRP78 significantly increased at 4, 12, 24, and 48 h of reperfusion. *In vivo*, expression of GRP78 in the affected side was significantly increased at 24 h and 48 h of reperfusion compared with the normal side (Fig. 5C).

3.4 Expression of estrogen receptors was suppressed during hypoxia-ischemia

The estrogen receptor has two subunits, estrogen receptor α (ERα) and estrogen receptor β (ERβ). Expression of ERα and ERβ was detected by western blot analysis after OGD/R or HIE. OGD/R significantly

JPET Fast Forward. Published on February 18, 2016 as DOI: 10.1124/jpet.115.230359
This article has not been copyedited and formatted. The final version may differ from this version.

decreased levels of ERα and ERβ at the 4 h to 48 h time points compared with the control group (Fig. 6). In addition, HIE inhibited expression of ERα and ERβ in 7-day-old rats. At 0 h to 48 h after HIE, the levels of ERα were decreased in the affected side compared with the normal side, and at 0, 24, and 48 h after HIE, the levels of ERβ were decreased in the affected side (Fig.6).

3.5 NGR1 inhibited OGD-induced injury *in vitro* via estrogen receptors

Given that NGR1 is a phytoestrogen with estrogenic effects, we reexamined apoptosis and injury of primary cortical neurons to investigate whether NGR1 exerted protective effects through estrogen receptors. At 4 h and 24 h after reperfusion, ICI-182780 (0.1 μmol/L) pretreatment abolished the effect of NGR1 (10 μmol/L) (Fig. 7). In the ICI-182780 + NGR1 group, cell viability was lower (Fig. 7A, B), more LDH was released (Fig. 7C, D), and more apoptotic morphological changes were observed compared with the NGR1 group (Fig. 7E, F). With ICI-182780 (0.1 μmol/L) pretreatment alone, more LDH were released and more abnormal nucleus were appeared compared with the OGD group at 24 h.

3.6 An estrogen receptor inhibitor blocked neuroprotective effects of NGR1 *in vivo*

The effect of the estrogen receptor inhibitor ICI-182780 was examined using TTC staining. As shown in previous experiments, infarction areas in the NGR1 group (15 mg/kg•12 h) were decreased in size compared with those in the HIE group. However, when ICI-182780 (2 mg/kg) was given before NGR1 treatment, the protective effects of NGR1 on the brain were attenuated. More infarction areas were detected in the ICI-182780+NGR1 group than in the NGR1 group. ICI-182780 treated alone also can lead to obvious infarction than NGR1 group ($*p<0.05$), however compared with HIE group, there was no statistical differences (Fig. 8A, B).

HE staining revealed that compared with the sham HIE group, the HIE group showed hyperaemia, cellular edema and tissue raritas (Fig. 8C). NGR1 treatment (15 mg/kg•12 h) attenuated tissue damage, while ICI-182780 (2 mg/kg) blocked the protective effects of NGR1. In the NGR1 + ICI-182780 group, more shrunken neurons and

cellular edema were observed compared with NGR1 group. At the same time, oedematous neurons and tissue raritas were observed in ICI-182780 group. These results further suggest that the estrogen receptor inhibitor blocked the neuroprotective effects of NGR1.

HIE treatment induce increase of cell apoptosis, a lot of TUNEL-positive cells can be seen in HIE group, but less TUNEL-positive were appeared in NGR1group. NeuN and TUNEL staining of brain tissues showed that ICI-182780 (2 mg/kg) pretreatment strongly suppressed the neuroprotective effects of NGR1 (15 mg/kg•12 h) in the ischemic animals, as indicated by a profound attenuation in the number of NeuN-positive cells and an increase in the number of TUNEL-positive cells in the NGR1 + ICI-182780 group. In ICI-182780 group, the number of TUNEL-positive cells is higher than that in NGR1 group but not obviously higher than that in HIE group (Fig. 8D, E).

3.7 NGR1 down regulated GRP78 via estrogen receptors *in vitro* and *in vivo*

To investigate whether NGR1 (10 μmol/L *in vitro* or 15 mg/kg *in vivo*) down regulated GRP78 via estrogen receptors, primary cortical neurons and 7-day-old rats were pretreated with ICI-182780 (0.1 μmol/L *in vitro* or 2 mg/kg *in vivo*), and then treated with NGR1. Western blot analysis revealed that in primary cortical neurons, NGR1 treatment significantly decreased GRP78 levels and this effect was blocked by ICI-182780. At the same time, ICI-182780 pretreated alone also induced activation of GRP78, the expression of GRP78 in ICI-182780 group is higher than that in OGD/R group (Fig. 9A, B). In the HIE group, expression of GRP78 increased in the affected side, and NGR1 (15 mg/kg•12 h) attenuated GRP78 activation. Pretreatment with ICI-182780 before NGR1 treatment resulted in a higher level of GRP78 than in the NGR1 group. In ICI-182780 group, there were GRP78 activation in affected side but the expression of GRP78 in ICI-182780 group is not obvious higher than that in HIE group (Fig. 9C, D).

Immunofluorescence staining was performed to assess GRP78, NeuN, and nuclei in the cerebral cortex. As

showed in Fig. 9E, GRP78 was primarily expressed in the cytoplasm, and GRP78 immunodensity was markedly increased by HIE treatment and attenuated by NGR1 (15 mg/kg•12 h). In NGR1+ICI-182780 group, the expression of GRP78 is higher compared with NGR1 group. Pretreatment with ICI-182780 (2 mg/kg) significantly increased expression of GRP78 but did not affect localization of GRP78.

3.8 NGR1 suppressed OGD/R-induced ER stress *in vitro* and *in vivo*

As shown in Fig. 10, in primary cortical neurons under ER stress, 2 of the 3 independent branches of the ER stress-associated pathways, PERK and IRE1, were activated under OGD/R indicating that both sensed stress. At 24 h following OGD/R, there was a clear increase in phospho-PERK and phospho-IRE1α. Treatment with NGR1 (10 μmol/L) decreased levels of phospho-PERK and phospho-IRE1α, and the effect of NGR1 was blocked by ICI-182780 (Fig. 10A, B). In addition, expression levels of CHOP, ERO1α, and caspase-12 were up regulated in the OGD group. NGR1 significantly decreased levels of these stress-associated proteins, and this effect was abolished by pretreatment with ICI-182780 (0.1 μmol/L) (Fig. 10A, B). BCL-2 is an inhibitor of apoptotic proteins, and NGR1 activated BCL-2. However, in the NGR1 + ICI-182780 group, the expression level of BCL-2 was as low as that in the OGD/R group. Pretreatment of ICI-182780 activated ER stress associated apoptotic protein (phospho-PERK , phospho-IRE1α, CHOP, ERO1α) and inhibit the expression of BCL-2. The expression of CHOP and ERO1α in ICI-182780 group is higher than that in OGD/R group (Fig. 10A, B).

HIE was established in 7-day-old rats and NGR1 (15 mg/kg•12 h) or ICI-182780 (2 mg/kg) was administered to rats through intraperitoneal injections. Expression levels of ER stress-related proteins were measured by western blot, and band densities for indicated proteins in the affected side were normalized to densities in the normal side and expressed as fold change. As shown in Fig. 11A, HIE stimulated expression of phospho-PERK, phospho-IRE1α, and CHOP. Treatment with NGR1 (15 mg/kg•12 h) decreased levels of phospho-PERK, phospho-IRE1α, and CHOP, while ICI-182780 pretreatment significantly attenuated the effects of

NGR1. NGR1 stimulated the level of BCL-2 in the affected side and ICI-182780 blocked this effect. ICI-182780 treatment alone could stimulate the expression of phospho-PERK, phospho-IRE1α, CHOP. Phospho-PERK in ICI-182780 group is higher than that in HIE group but there was no statistic difference.

Discussion

Panax notoginseng, is believed to have anti-inflammatory, anti-oxidative, and anti-apoptotic properties (Liu et al., 2010; Li et al., 2014). In Zhang study, NGR1 could attenuate inflammatory bowel disease via the pregnane X receptor (Zhang et al., 2015), NGR1 also can alleviate inflammation-induced cardiomyocyte injury through attenuated the activation of NF-κB (Zhong et al., 2015). NGR1 has neuroprotective in adults through down-regulated expression of aquaporin 4 or restored the elevation of elevation of LC3 and Beclin 1 (Zhou et al., 2013; Lu et al., 2011). However, neuroprotective properties and underlying mechanisms of NGR1during HIE in newborns are largely unknown, due to the uniqueness of the neonatal brain (Hansen et al., 2004). ER stress plays an important role in HIE, and ER stress can be mediated by estrogen. In this study, we designed a series of experiments to clarify whether the anti-apoptotic effects of NGR1 ameliorated ER stress induced by cell and brain injury under hypoxic-ischemic conditions. The principal findings in the present study are as follows: (1) During progression of HIE, ER stress is activated and estrogen receptors and are suppressed. (2) NGR1 significantly attenuates brain dysfunction in primary cortical neurons and 7-day-old rats by blocking activation of ER stress via estrogen receptors.

HIE is a common neurological disease in newborns. Although the exact pathophysiology of HIE is not completely understood, apoptosis is one of the major pathways that lead to neuronal death after cerebral hypoxia-ischemia (Zhu et al., 2003). By assessing apoptosis of cells and injury to brain tissue, this study found that NGR1 exerted neuroprotection under HIE conditions both *in vitro* and *in vivo*. This conclusion is based on the findings that at 4 h or 24 h of OGD/R, 24 h after HIE, NGR1 significantly decreased cell injury. Similar results were found by Meng (Meng et al., 2014), however, the effective concentrations of NGR1 used in our study (10 μmol/L *in vitro* and 15 mg/kg *in vivo*) were lower than those used in the Meng study (25 μmol/L *in vitro* and 20 mg/kg *in vivo*). The difference may be because we used cells on day 5 of culture and 7-day-old rats, rather than

JPET Fast Forward. Published on February 18, 2016 as DOI: 10.1124/jpet.115.230359
This article has not been copyedited and formatted. The final version may differ from this version.

cells on day 7 of culture or adult rats. In addition, in our study, NGR1 was administered after OGD or surgery rather than as a pretreatment.

NGR1 is phytoestrogen which can regulate Akt/Nrf2 pathways or TNF-α via estrogen receptor (Lei et al.,2015; Meng et al., 2014). Two important subtype of estrogen receptor, ERα and ERβ are transcription factors which could activate and regulate cell survival, growth and metabolism through modulation of gene expression (Qin et al., 2015). Such as ICI-182780 is a blocker of ERα and ERβ, and the optimal concentration of the NGR1 on neuron cells is 0.1 μmol/L (Meng et al., 2014) and IC50 of ICI-182780 on cancer cells is 0.29 nmol/L (Alan et al., 1991). All above suggest that NGR1 may come into play through estrogen receptors.

Recent advances have highlighted the importance of ER stress during HIE (Xinzhi Chen et al., 2008; Zhao et al., 2015). ER stress contributes to many cellular processes involving protein folding and Ca^{2+} homeostasis, deploys a series of regulatory mechanisms in response to stress (Cao et al., 2015). ER stress can also activate cell apoptosis signals, which result in cell apoptosis and deterioration of neurological symptoms. UPR is an intracellular signal transduction pathway that monitors ER homeostasis (Wu et al., 2014). Perturbation of the UPR may contribute to many diseases, including neurodegenerative disorders (Matus et al., 2011), metabolic diseases (Usui et al., 2012), and inflammation (Kaser et al., 2011). GRP78 is an important molecular chaperone in ER stress, and treatments that stimulate the UPR in the ER increase expression of GRP78 (Kozutsumi et al., 1988). In primary cortical neurons or 7-day-old rats, our study show that OGD/R or HIE clearly increased expression of GRP78 (Fig. 5) and NGR1 could inhibit the expression of GRP78, *in vitro* or *in vivo* (Fig. 9). Results show that HIE could initiate ER stress in neonatal brain, it is consistent with Badiola study (Badiola et al., 2011), and furthermore, it proved that NGR1 clearly blocked activation of ER stress.

Estrogen receptors play an important role in the ER stress process, and there is a link between the UPR and estrogen signaling (Raina et al., 2014). Stimulation of estrogen receptors can reduce ER stress to protect against

glucotoxicity-induced pancreatic cell death (Kooptiwu et al., 2014). HIE could influence the ontogenesis of brain μ-opioid receptors then lead to down-regulation of estrogen receptors (Kraczkowski et al., 2000). Our results show that ERα and ERβ receptor expression was reduced during neuronal ischemic (Fig. 6), the result was same with Marcelo (Marcelo et al., 2008) and our results show decreasing of ERα and ERβ was associated with activating of ER stress (Fig. 10, 11). NGR1 is an estrogen receptor agonist (Sun et al., 2013; Gui et al., 2014) which can regulate the NF-κB (Zhong L et al., 2015) or autophagy (Zhou et al., 2013; Lu et al., 2011) via estrogen receptor under the pathological circumstance. In the neuronal ischemic case,NGR1 action on ERα and ERβ as an agonist to strengthen the role of ERα and ERβ then attenuates the ER stress. As shown in Figures (Fig.7 to 11), serious cells and brain injury were observed in the ICI-182780 + NGR1 group compared with the NGR1 group. Blocking estrogen receptors before NGR1 treatment also could upregulate the related proteins expression of ER stress and apoptosis. Thus, all these data confirmed that NGR1 stimulate the ERα and ERβ to attenuate the ER stress and then protected the brain from ER stress.

To examine further the influence of NGR1 on ER stress-induced apoptosis, we measured expression levels of GRP78 downstream signaling molecules. Stress causes protein misfolding in the ER, and their accumulation induces synthesis of GRP78, which eliminates unfolded proteins and maintains ER homeostasis. However, the UPR has limitations; when ER stress is too strong or too long in duration and ER homeostasis cannot be restored, the accumulation of unfolded proteins in the ER induces dissociation of the ER chaperone GRP78 from three ER transmembrane effector proteins: RNA-activated protein kinase-like ER kinase (PERK), inositol requiring kinase 1 (IER1), and transcription factor 6 (ATF6) (Hetz et al., 2011). PERK recognizes the UPR via its luminal sensor/transducer domain. Activated PERK and subsequent activation of CHOP and ERO1 are essential for ER stress-induced apoptosis. CHOP and ERO1 can further activate the mitochondrial apoptosis pathway (Tabas et al., 2011). Caspase-12 is localized to the endoplasmic reticulum lumen, and is considered the initiator of ER

stress-mediated caspase signal pathway (Fischer et al., 2002; Saleh et al., 2006). The transmembrane IRE1 dimerizes, leading to splicing of X-box binding protein 1 (XBP1) mRNA to produce an altered reading frame. The JNK cell apoptosis pathway then becomes activated, and JNK can inhibit expression of BCL-2 (Muscarella et al., 2008), which is an inhibitor of apoptosis proteins. Activated ATF6, which mainly plays a role in promoting survival, it is proteolytically cleaved in the Golgi apparatus and promotes transcription of ER chaperones in the nucleus (Adachi et al., 2008). Therefore, we evaluated expression levels of GRP78 downstream signaling molecules and apoptosis-related proteins including phospho-PERK, CHOP, ERO1α, caspase-12, phospho-IRE1α, and BCL-2. Our *in vivo* and *in vitro* results revealed that HIE was accompanied by stimulation of ER stress-associated apoptosis-related proteins, these results are similar to those in a study by Zhao (Zhao et al., 2015). NGR1 could relieve the expression of apoptosis-related proteins. However, ICI-182780 significantly blocked the effects of NGR1 (Fig.7, 8, 9). These data suggest that NGR1 attenuates OGD- or HIE-induced activation of ER stress, and that NGR1 exerts its protective effects via estrogen receptors. In vitro study, ICI-182780 treat alone will exacerbate the stress response. However in vivo study, ICI-182780 alone could not increase the injury obviously as the result in vitro study. That may because of the autoregulation of endocrine factors in animals; the damage effect of ICI-182780 on animals was decreased (Davis et al., 2008, Chakraborty et al., 2004).

In summary, the present study demonstrated that the neuroprotective mechanisms of NGR1 involve estrogen receptor-dependent suppression of ER stress. (Fig. 12). After ischemia-hypoxia, PERK and IRE1 are activated and sequentially promote expression of CHOP, ERO1, and caspase-12, and suppress BCL-2 signaling pathways. Activation of PERK and IRE1 eventually results in cell apoptosis. NGR1 targets estrogen receptors and inhibits activation of PERK and IRE1. Our findings offer a novel treatment strategy for targeting ER stress, and NGR1 might be used as a strategy for treatment of neonatal HIE injury.

Acknowledgements

We thank LetPub (www.letpub.com) for its linguistic assistance during the preparation of this manuscript.

Authorship Contributions

Participated in research design: Yan Wang, Shali Wang

Conducted experiments: Yan Wang, Liu Tu, Di Chen, Yingbo Li

Contributed new reagents or analytic tools: Yan Wang, Liu Tu

Performed data analysis: Di Chen, Yingbo Li

Wrote or contributed to the writing of the manuscript: Yan Wang, Liu Tu, Di Chen, Yingbo Li, Shali Wang

References

Adachi Y, Yamamoto K, Okada T, Yoshida H, Harada A, Mori K (2008) ATF6 is a transcription factor specializing in the regulation of quality control proteins in the endoplasmic reticulum. Cell Struct Funct 33:75-89

Alan E, Wakeling, Michael Dukes, Jean Bowler (1991) A Potent Specific Pure Antiestrogen with Clinical Potential. Cancer research 51: 3867-3873

Badiola N, Penas C, Miñano-Molina A, Barneda-Zahonero B, Fadó R, Sánchez-Opazo G, Comella JX, Sabriá J, Zhu C, Blomgren K, Casas C, Rodríguez-Alvarez J (2011) Induction of ER stress in response to oxygen-glucose deprivation of cortical cultures involves the activation of the PERK and IRE-1 pathways and of caspase-12. Cell Death and Disease 2:e149

Bing Sun, Jing Xiao, Xiao-Bo Sun and Ying Wu (2013) Notoginsenoside R1attenuates cardiac dysfunction in endotoxemic mice: an insight into oestrogen receptor activation and PI3K/Akt signalling. British Journal of Pharmacology 168:1758–1770;

Cao SS, Luo KL, Shi L (2015) Endoplasmic Reticulum Stress Interacts with Inflammation in Human Diseases. J Cell Physiol 22: 900-918

Chakraborty, Gore (2004) Aging-related changes in ovarian hormones, their receptors, and neuroendocrine function. Exp. Biol. Med 229: 977–987

Chan RY, Chen WF, Dong A, Guo D, Wong MS (2002) Estrogen-like activity of ginsenoside Rg1 derived from Panax notoginseng. J Clin Endocrinol Metab 87:3691-3695

Chen X, Kintner DB, Luo J, Baba A, Matsuda T, Sun D (2008) Endoplasmic reticulum Ca^{2+} dysregulation and endoplasmic reticulum stress following in vitro neuronal ischemia: role of Na^{+}-K^{+}-Cl^{-} cotransporter. J Neurochem 106: 1563–1576

Chi W, Meng F, Li Y, Li P, Wang G, Cheng H, Han S, Li J (2014) Impact of microRNA-134 on neural cell

survival against ischemic injury in primary cultured neuronal cells and mouse brain with ischemic stroke by targeting HSPA12B. Brain Res 1592:22-33

Davis AM, Mao J, Naz B, Kohl JA, Rosenfeld CS (2008) Comparative effects of estradiol, methyl-piperidino-pyrazole, raloxifene, and ICI 182 780 on gene expression in the murine uterus. J Mol Endocrinol 41:205–217.

Doroudgar S, Glembotski CC (2013) ATF6 [corrected] and thrombospondin 4: the dynamic duo of the adaptive endoplasmic reticulum stress response. Circ Res 112: 9-12

Fischer H, Koenig U, Eckhart L, Tschachler E (2002) Human caspase 12 has acquired deleterious mutations. Biochem Biophys Res Commun 293:722-726

Gui D, Wei L, Jian G, Guo Y, Yang J, Wang N (2014) Notoginsenoside R1 ameliorates podocyte adhesion under diabetic condition through α3β1 integrin upregulation in vitro and in vivo. Cell Physiol Biochem. 34:1849-1862

Hammadi M, Oulidi A, Gackière F, Katsogiannou M, Slomianny C, Roudbaraki M, Dewailly E, Delcourt P, Lepage G, Lotteau S, Ducreux S, Prevarskaya N, Van Coppenolle F (2013) Modulation of ER stress and apoptosis by endoplasmic reticulum calcium leak via translocon during unfolded protein response: involvement of GRP78. FASEB J 27:1600-1609

Han jinan, Hu weiyi (1996) Protective effect of Notoginseng on the ischemic brain injury. Chinese Journal of Integrated Traditional and Western Medicine 8: 506-507

Hansen HH, Briem T, Dzietko M, Sifringer M, Voss A, Rzeski W, Zdzisinska B, Thor F, Heumann R, Stepulak A, Bittigau P, Ikonomidou C (2004) Mechanisms leading to disseminated apoptosis following NMDA receptor blockade in the developing rat brain. Neurobiol Dis 16:440-453

Hayashi T, Saito A, Okuno S, Ferrand-Drake M, Dodd RL, Chan PH (2005) Damage to the endoplasmic

reticulum and activation of apoptotic machinery by oxidative stress in ischemic neurons. J Cereb Blood Flow Metab 25: 41–53

Hetz C, Martinon F, Rodriguez D, Glimcher LH (2011) The unfolded protein response: integrating stress signals through the stress sensor IRE1α. Physiol Rev 91:1219-1243

Jayakara Shetty (2015) Neonatal seizures in hypoxic–ischaemic encephalopathy – risks and benefits of anticonvulsant therapy. Developmental Medicine & Child Neurology 57:40–43

Jiabin Guo, Sue P. Duckles, John H. Weiss1, Xuejun Li, and Diana N. Krause (2012) 17β-Estradiol prevents cell death and mitochondrial dysfunction by estrogen receptor-dependent mechanism in astrocytes following oxygen-glucose deprivation/reperfusion. Free Radic Biol Med 52: 2151–2160

Kaser A, Flak MB, Tomczak MF, Blumberg RS (2011) The unfolded protein response and its role in intestinal homeostasis and inflammation. Exp Cell Res 317 :2772-2779

Kooptiwut S, Mahawong P, Hanchang W, Semprasert N, Kaewin S, Limjindaporn T, Yenchitsomanus PT (2014) Estrogen reduces endoplasmic reticulum stress to protect against glucotoxicity induced-pancreatic β-cell death. J Steroid Biochem Mol Biol 139:25-32

Kozutsumi Y, Segal M, Normington K, Gething MJ, Sambrook J (1988) The presence of malfolded proteins in the endoplasmic reticulum signals the induction of glucose-regulated proteins. Nature 332:462-464

Kraczkowski, M. Semczuk (2000) Sex and changes in mu-opioid receptor density under hypoxia. Ginekol. Pol 71: 927–930

Lakshmanan AP, Thandavarayan RA, Palaniyandi SS, Sari FR, Meilei H, Giridharan VV, Soetikno V, Suzuki K, Kodama M, Watanabe K (2011) Modulation of AT-1R/CHOP-JNK-Caspase12 pathway by olmesartan treatment attenuates ER stress-induced renal apoptosis in streptozotocin-induced diabetic mice. Eur J Pharm Sci 44:627-634

Lei Z, Xing LZ, Yan SL, Yi MW, Fei M, Bao LG, Zhao QY, Qing YZ (2015) Estrogen receptor α mediates the

effects of notoginsenoside R1 on endotoxin-induced inflammatory and apoptotic responses in H9c2 cardiomyocytes. Molecular medicine reports 12: 119-126

Li C, Li Q, Liu YY, Wang MX, Pan CS, Yan L, Chen YY, Fan JY, Han JY (2014) Protective effects of Notoginsenoside R1 on intestinal ischemia-reperfusion injury in rats. Am J Physiol Gastrointest Liver Physiol 306: G111-22

Li G, Mongillo M, Chin KT, Harding H, Ron D, Marks AR, Tabas I (2009) Role of ERO1-mediated stimulation of inositol 1,4,5-triphosphate receptor activity in endoplasmic reticulum stress–induced apoptosis . J Cell Biol 186:783-792

Li SS, Ye JM, Deng ZY, Yu LX, Gu XX, Liu QF (2015) Ginsenoside-Rg1 inhibits endoplasmic reticulum stress-induced apoptosis after unilateral ureteral obstruction in rats. Ren Fail 24:1-6

Liu QF, Deng ZY, Ye JM, He AL, Li SS (2015) Ginsenoside Rg1 protects chronic cyclosporin a nephropathy from tubular cell apoptosis by inhibiting endoplasmic reticulum stress in rats. Transplant Proc 47:566-569

Liu WJ, Tang HT, Jia YT, Ma B, Fu JF, Wang Y, Lv KY, Xia ZF (2010) Notoginsenoside R1 attenuates renal ischemia-reperfusion injury in rats. Shock 34: 314–320

Liu Y, Du FY, Chen W, Fu PF, Yao MY, Zheng SS (2015) G15 sensitizes epithelial breast cancer cells to doxorubicin by preventing epithelial-mesenchymal transition through inhibition of GPR30. Am J Transl Res 7:967-975.

Lu T, Jiang Y, Zhou Z, Yue X, Wei N, Chen Z, Ma M, Xu G, Liu X (2011) Intranasal ginsenoside Rb1 targets the brain and ameliorates cerebral ischemia/reperfusion injury in rats. Biol Pharm Bull 34:1319 -1324

Marcelo E, Ezque, Susana R. Valdeza, Alicia M. Seltzerb, Graciela A. Jahna (2008) Advancement of reproductive senescence and changes in the early expression of estrogen, progesterone and μ-opioid

receptors induced by neonatal hypoxia in the female rat. Brain research 1214: 73–83

Matus S, Glimcher LH, Hetz C (2011) Protein folding stress in neurodegenerative diseases: a glimpse into the ER. Curr Opin Cell Biol 23:239-252

Meng X, Wang M, Wang X, Sun G, Ye J, Xu H, Sun X (2014) Suppression of NADPH oxidase- and mitochondrion-derived superoxide by Notoginsenoside R1 protects against cerebral ischemia-reperfusion injury through estrogen receptor-dependent activation of Akt/Nrf2 pathways. Free Radic Res 48:823-838

Mirza MA, Ritzel R, Xu Y, McCullough LD, Liu F (2015) Sexually dimorphic outcomes and inflammatory responses in hypoxic-ischemic encephalopathy. J Neuroinflammation 12 :32

Mo H, Chen Y, Huang L, Zhang H, Li J, Zhou W (2013) Neuroprotective effect of tea polyphenols on oxyhemoglobin induced subarachnoid hemorrhage in mice. Oxid Med Cell Longev 2013:743938

Muscarella DE, Bloom SE (2008) T The contribution of c-Jun N-terminal kinase activation and subsequent Bcl-2 phosphorylation to apoptosis induction in human B-cells is dependent on the mode of action of specific stresses. Toxicol Appl Pharmacol 228:93-104

Northington FJ, Chavez-Valdez R, Martin LJ (2011) Neuronal cell death in neonatal hypoxia-ischemia. Ann Neurol 69 :743-758

Poone GK, Hasseldam H, Munkholm N, Rasmussen RS, Grønberg NV, Johansen FF (2015)The Hypothermic Influence on CHOP and Ero1-α in an Endoplasmic Reticulum Stress Model of Cerebral Ischemia. Brain Sci 5:178-187

Qin PS, Fan LJ, Zhu JJ (2000) Clinical research of danshen dropping pills for coronary atherosclerotic heart disease. Chinese patent medicine 22: 630

Qin Xue, Daliao Xiao, and Lubo Zhang. (2015) Estrogen regulates angiotensin II receptor expression patterns and protects the heart from ischemic injury in female rats. BOR Papers in Press. Published on May 13,

2015

Raina K, Noblin DJ, Serebrenik YV, Adams A, Zhao C, Crews CM (2014) Targeted protein destabilization reveals an estrogen-mediated ER stress response. Nat Chem Biol 10:957-962

Rao RV, Ellerby HM, Bredesen DE (2004) Coupling endoplasmic reticulum stress to the cell death program. Cell Death Differ 11: 372–380

Raval AP, Bramlett H, Perez-Pinzon MA (2006) Estrogen preconditioning protects the hippocampal CA1 against ischemia. Neuroscience 141:1721–1730

Saleh M, Mathison JC, Wolinski MK, Bensinger SJ, Fitzgerald P, Droin N, Ulevitch RJ, Green DR, Nicholson DW (2006) Enhanced bacterial clearance and sepsis resistance in caspase-12-deficient mice. Nature 440:1064-1068

Sun B, Xiao J, Sun XB, Wu Y (2013) Notoginsenoside R1 attenuates cardiac dysfunction in endotoxemic mice: an insight into oestrogen receptor activation and PI3K/Akt signaling. British Journal of Pharmacology 168: 1758–1770

Sun DS, Chang HH (2003) Differential regulation of JNK in caspase-3-mediated apoptosis of MPP(+)-treated primary cortical neurons. Cell Biol 27:769–777

Sun Genyi，Zhang Ying，W u W ei，Liu Ting (2011) On Compound Danshen Dripping Pill for Treatment of 214 CHD patients with Aspirin Resistance. World Chinese Medicine 6: 301-302

Tabas I, Ron D (2011) Integrating the mechanisms of apoptosis induced by endoplasmic reticulum stress. Nat Cell Biol 13:184-190

Usui M, Yamaguchi S, Tanji Y, Tominaga R, Ishigaki Y, Fukumoto M, Katagiri H, Mori K, Oka Y, Ishihara H (2012) Atf6α-null mice are glucose intolerant due to pancreatic β-cell failure on a high-fat diet but partially resistant to diet-induced insulin resistance. Metabolism 61:1118-1128

Wang T, Li Y, Wang Y, Zhou R, Ma L, Hao Y, Jin S, Du J, Zhao C, Sun T, Yu J (2014) Lycium barbarum Polysaccharide Prevents Focal Cerebral Ischemic Injury by Inhibiting Neuronal Apoptosis in Mice. PLoS One 9:e90780

Wu H, Ng BS, Thibault G (2014) Endoplasmic reticulum stress response in yeast and humans. Biosci Rep 34 : e00118

Xinzhi Chen, Douglas B. Kintner, Jing Luo, Akemichi Baba, Toshio Matsuda, Dandan Sun (2008) ER Ca^{2+} dysregulation and ER stress following in vitro neuronal ischemia: role of Na^{+}-K^{+}-Cl^{-} cotransporter. J Neurochem 106: 1563–1576

Xu C, Bailly-Maitre B, Reed JC (2005) Reed Endoplasmic reticulum stress: cell life and death decisions. J Clin Invest 115:2656-2664

Zhang J, Ding L, Wang B, Ren G, Sun A, Deng C, Wei X, Mani S, Wang Z, Dou W (2015) Notoginsenoside R1 attenuates experimental inflammatory bowel disease via pregnane X receptor activation. J Pharmacol Exp Ther 352:315-324)

Zhang YJ (2001) Effect of danshen dropping pills on hyperlipemia. Jing zhou yi xue yaun bao 22:36

Zhao H, Wang R, Wu X, Liang J, Qi Z, Liu X, Min L, Ji X, Luo Y (2015) Erythropoietin delivered via intra-arterial infusion reduces endoplasmic reticulum stress in brain microvessels of rats following cerebral ischemia and reperfusion. J Neuroimmune Pharmacol 10: 153-161

Zhao J, Shi Z, Liu S, Li J, Huang W (2014) Ginsenosides Rg1 from Panax ginseng: A Potential Therapy for Acute Liver Failure Patients? Evid Based Complement Alternat Med 2014:538059

Zhong L, Zhou XL, Liu YS, Wang YM, Ma F, Guo BL, Yan ZQ, Zhang QY (2015) Estrogen receptor α mediates the effects of notoginsenoside R1 on endotoxin-induced inflammatory and apoptotic responses in H9c2 cardiomyocytes . Mol Med Rep 12:119-126

Zhou Y, Li HQ, Lu L, Fu DL, Liu AJ, Li JH, Zheng GQ (2013) Ginsenoside Rg1 provides neuroprotection against blood brain barrier disruption and neurological injury in a rat model of cerebral ischemia/reperfusion through downregulation of aquaporin 4 expression. Phytomedicine 21:998-1003

Zhu C, Qiu L, Wang X, Hallin U, Candé C, Kroemer G, Hagberg H, Blomgren K (2003) Involvement of apoptosis-inducing factor in neuronal death after hypoxia-ischemia in the neonatal rat brain. J Neurochem 86: 306-317

Zhu C, Wang X, Xu F, Bahr BA, Shibata M, Uchiyama Y, Hagberg H, Blomgren K (2004) The influence of age on apoptotic and other mechanisms of cell death after cerebral hypoxia-ischemia. Cell Death Differ 12: 162–176

Footnotes

This study was supported by the National Natural Science Foundation of China (81401234).

Shali Wang, Institute of neuroscience, Chongqing Medical University, Chongqing, China.

Legends for Figures

Fig. 1. The molecular structure of NGR1

Fig. 2.Effect of NGR1on neurons during sham-OGD case

(A and B) MTT assays showed that NGR1 (0.5, 1, 2, 5, 10, and 20 μmol/L) did not affect cell viability at 4 h and 24 h after sham OGD. (C and D) Measurements of LDH release showed that NGR1 (0.5, 1, 2, 5, 10, and 20 μmol/L) did not damage cell integrity. At 4 h and 24 h after sham OGD, LDH release in the NGR1 group was the same as that in the sham-OGD group. (#p>0.05, significant without differences, compared with groups, n = 5), Mean + SD.

Fig. 3. Concentration-dependent effects of NGR1 on cell injury at 4 h and 24 h after OGD/R

(A) NGR1 (10, 20 μmol/L) increased cell viability 4 h after OGD/R compared with the OGD/R group. (B) At 24 h after OGD/R, NGR1 (5, 10, and 20 μmol/L) still increased cell viability. (C and D) NGR1 (5, 10, and 20 μmol/L) reduced LDH release. (E and F) NGR1 (10 μmol/L) treatment attenuated OGD-induced morphological changes of nuclei. Scale bar = 200 μm. (*p<0.05 compared with groups, n = 5), Mean + SD.

Fig. 4. Effect of NGR1 on brain injury after HIE

(A) Photomicrographs of TTC-stained coronal slices showing brain infarction 24 h after HIE. Scale bar = 1 cm. (B) NGR1 exerted neuroprotective effects and 15 mg/kg•12 h was the optimal dose. (C) Photomicrographs of HE-stained coronal slices. Black arrows indicate oedematous cells. Scale bar = 200 μm. (D, E) After HIE treatment, many TUNEL-positive neurons were observed in the cerebral cortex, and NGR1 (10 mg/kg) decreased the number of TUNEL-positive neurons. Scale bar = 200 μm. (*p<0.05 compared with groups, n = 4–5 rats), Mean + SD.

Fig. 5. Effect of hypoxia ischemia on expression of GRP78 *in vitro* and *in vivo*

(A) Representative western blots for GRP78 in primary cortical neurons. (B) At 4 h to 48 h after reoxygenation, expression of GRP78 was significantly increased. (C) Representative western blots for GRP78 in HIE rats. (D) Compared with the normal side, GRP78 was expressed at a high level in the affected side at 0, 24, and 48 h after HIE. (*$p<0.05$ compared with groups, n = 5 *in vitro*, n = 4–6 rats *in vivo*), Mean + SD.

Fig. 6. Expression of estrogen receptors during OGD/R and HIE

(A) Representative western blots for ERα and ERβ in primary cortical neurons. (B and C) ERα was expressed at low levels 4 h to 48 h after OGD/R, and ERβ was expressed at low levels 0 h to 48 h after OGD/R. (D) Representative western blots for ERα and ERβ in HIE rats. (E and F) Compared with the normal side, ERα and ERβ were expressed at low levels in the affected side at 0, 24, and 48 h after HIE. (*$p<0.05$ compared with groups, n = 5 *in vitro*, n = 4–6 rats *in vivo*), Mean + SD.

Fig. 7. Effect of estrogen receptor antagonist on cell injury

(A and B) At 4 h and 24 h after OGD/R, NGR1 (10 μmol/L) increased cell viability, while ICI-182780 (0.1 μmol/L) pretreatment abolished the NGR1 effect. Groups treated with NGR1+ICI-182780 (0.1 μmol/L) had lower cell viability compared with NGR1 group. In ICI-182780 group, there were lower cell viability than that in NGR1+ICI-182780 group, but there is no statistical differences (C and D) At 4 h and 24 h after OGD/R, NGR1 (10 μmol/L) reduced LDH release in neurons, and ICI-182780 (0.1 μmol/L) increased cell injury. In the 24h after OGD/R, higher LDH were released in ICI-182780 group than that in OGD group. (E and F) At 4 h and 24 h after OGD/R, ICI-182780 (0.1 μmol/L) suppressed the neuroprotective effects of NGR1 (10 μmol/L), with more

pyknotic or fragmented nuclei than in the NGR1 group. ICI-182780 (0.1 μmol/L) pretreatment alone also lead to obvious cell apoptosis at 24 h. Scale bar = 200 μm (*p<0.05 compared with groups, n = 5), Mean + SD.

Fig. 8. Effect of estrogen receptor antagonist on brain injury

(A) Photomicrographs of TTC-stained coronal slices showing brain infarction 24 h after HIE. Scale bar = 1 cm. (B) NGR1 (15 mg/kg•12 h) reduced infarction area, but NGR1+ICI-182780 (2 mg/kg) group have larger infarction area that in NGR1 group. ICI-182780 alone can cause serious brain infarction but has no statistical differences with HIE group. ICI: ICI-182780 (C) Compared with the NGR1 (15 mg/kg•12 h) group, ICI-182780 (2 mg/kg) enhanced cell injury, tissue raritas and the cellular edema (indicated by black arrows) both in NGR1+ICI-182780 and ICI-182780 group, scale bar = 200 μm. (D, E) The number of TUNEL-positive neurons was greater in the NGR1+ICI-182780 group (2 mg/kg) than in the NGR1 (15 mg/kg•12 h) group. A lot of TUNEL-positive neurons in ICI-182780 group but the number of TUNEL-positive cells in ICI-182780 group does not obviously higher than that in HIE group. Scale bar = 200 μm. (*p <0.05 compared with groups, n = 4–5 rats), Mean + SD

Fig. 9. Effect of NGR1 on expression of GRP78 in cases of hypoxia-ischemia *in vitro* and *in vivo*

(A) Representative western blots for GRP78 in primary cortical neurons. (B) In primary cortical neurons, NGR1 (10 μmol/L) inhibited an increase in GRP78 and ICI-182780 (0.1 μmol/L) promoted GRP78 activation. Expression of GRP78 in NGR1+ ICI-182780 is higher than that in NGR1 group, and GRP78 in ICI-182780 is higher than that in OGD/R group. (C) Representative western blots for GRP78 in HIE rats. (D) Compared with the normal side, NGR1 (15 mg/kg•12 h) attenuated HIE-induced GRP78 upregulation, while ICI-182780 (2 mg/kg) abolished the effect of NGR. ICI-182780 treat alone do not aggravate the expression of GRP78 compared with HIE group. ICI: ICI-182780 (E) Representative immunofluorescence staining of the cerebral cortex showing GRP78 (red), NeuN

JPET Fast Forward. Published on February 18, 2016 as DOI: 10.1124/jpet.115.230359
This article has not been copyedited and formatted. The final version may differ from this version.

(green), and nuclei (blue). Scale bar = 200 μm (*p<0.05 compared with groups, n = 5 *in vitro*, n = 4–6 rats *in vivo*), Mean + SD.

Fig. 10. Effect of NGR1 and ICI-182780 on ER stress during OGD/R *in vitro*

(A and B) Western blot analysis of phospho-PERK, PERK, CHOP, caspase-12, cleaved-caspase-12, ERO1-α, phospho-IRE1α, IRE1α, and BCL-2 in primary cortical neurons. (C-H) NGR1 (10 μmol/L) suppressed expression of phospho-PERK, CHOP, cleaved-caspase-12, ERO1-α, and phospho-IRE1α, and increased expression of BCL-2. In NGR1+ICI-182780 group, expression of phospho-PERK, CHOP, cleaved-caspase-12, ERO1-α, phospho-IRE1α was increased and BCL-2 was decreased compared with NGR1 group. ICI-182780 (0.1 μmol/L) treatment alone led to activation of phospho-PERK, CHOP, cleaved-caspase-12, ERO1-α, phospho-IRE1α and inhibition of BCL-2. The expression of CHOP and ERO1α in ICI-182780 group is higher than that in OGD/R group. ICI: ICI-182780 (0.1 μmol/L) (*p<0.05 compared with groups, n = 5), Mean + SD.

Fig. 11. Effect of NGR1 and ICI-182780 on ER stress during OGD/R *in vivo*

(A) Western blot analysis of phospho-PERK, PERK, phospho-IRE1α, IRE1α, CHOP, and BCL-2 *in vivo*. (B-E) NGR1 (15 mg/kg•12 h) inhibited increases in phospho-PERK, phospho-IRE1α, and CHOP, and enhanced expression of BCL-2. In the NGR1 + ICI-182780 (2 mg/kg) group, we detected higher levels of phospho-PERK, phospho-IRE1α, and CHOP, and a lower level of BCL-2 in affected side. ICI-182780 treatment alone led to activation of phospho-PERK, CHOP, phospho-IRE1α and inhibition of BCL-2 but no statistical difference with the HIE. ICI: ICI-182780 (*p<0.05 compared with groups, n = 4–6 rats *in vivo*), Mean + SD.

Fig. 12. Scheme of mechanisms underlying attenuation of ER stress induced by hypoxic-ischemic, after

NGR1 treatment.

Hypoxia-ischemia stimulates ER stress and results in activation of PERK and IRE1. Phospho-PERK triggers activation of CHOP, ERO1, and caspase-12, all of which induce mitochondria-associated apoptosis. Phospho-IRE1 activates the JNK pathway, inhibits BCL-2, and promotes apoptosis through mitochondria. Phospho-ATF6 plays a survival role through the Golgi body. NGR1 activates estrogen receptors and inhibits activation of phospho-PERK and phospho-IRE1. The estrogen receptor inhibitor ICI-182780 inhibits the interaction between NGR1 and estrogen receptors.

JPET Fast Forward. Published on February 18, 2016 as DOI: 10.1124/jpet.115.230359
This article has not been copyedited and formatted. The final version may differ from this version.

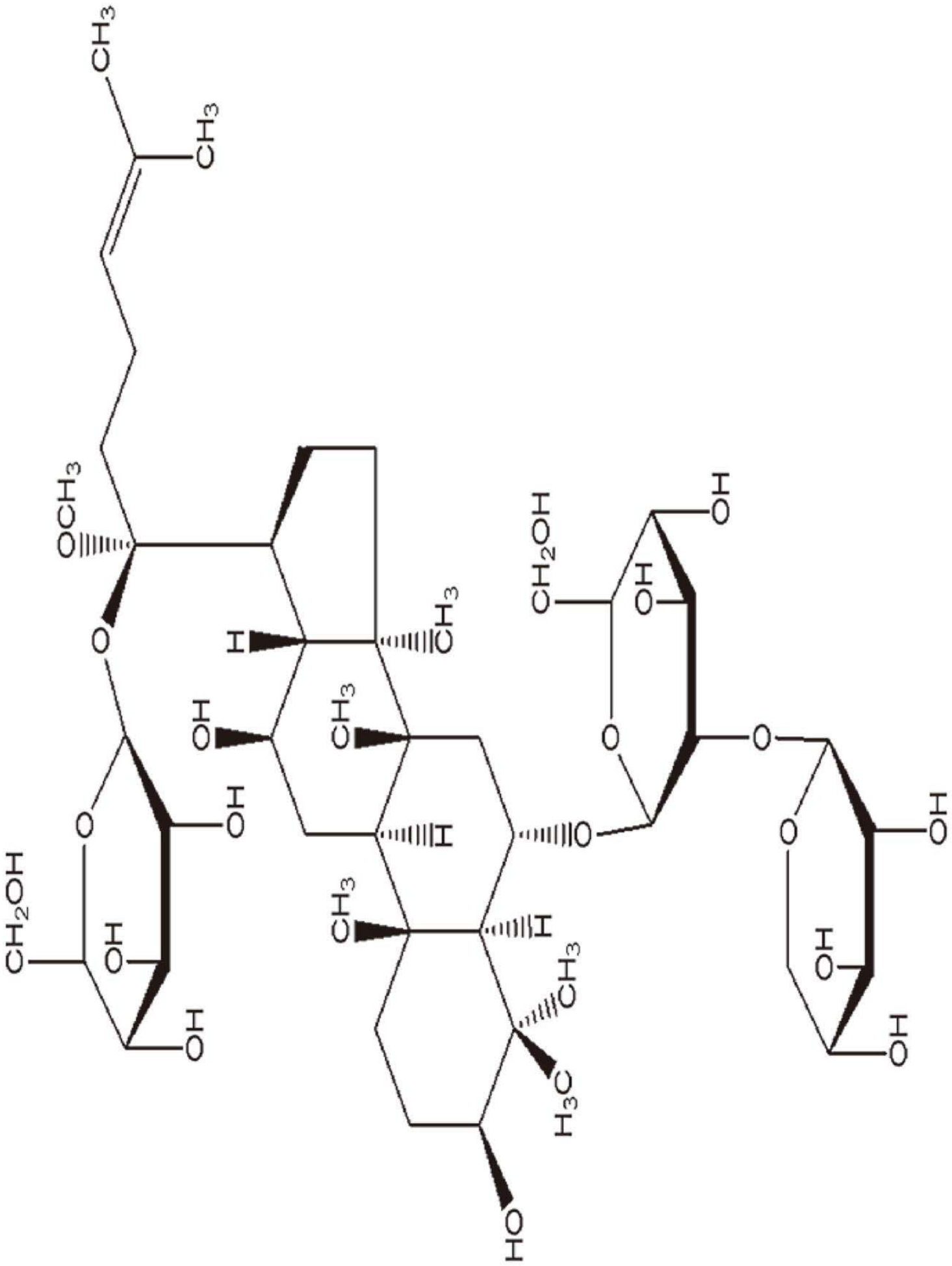

Fig. 1

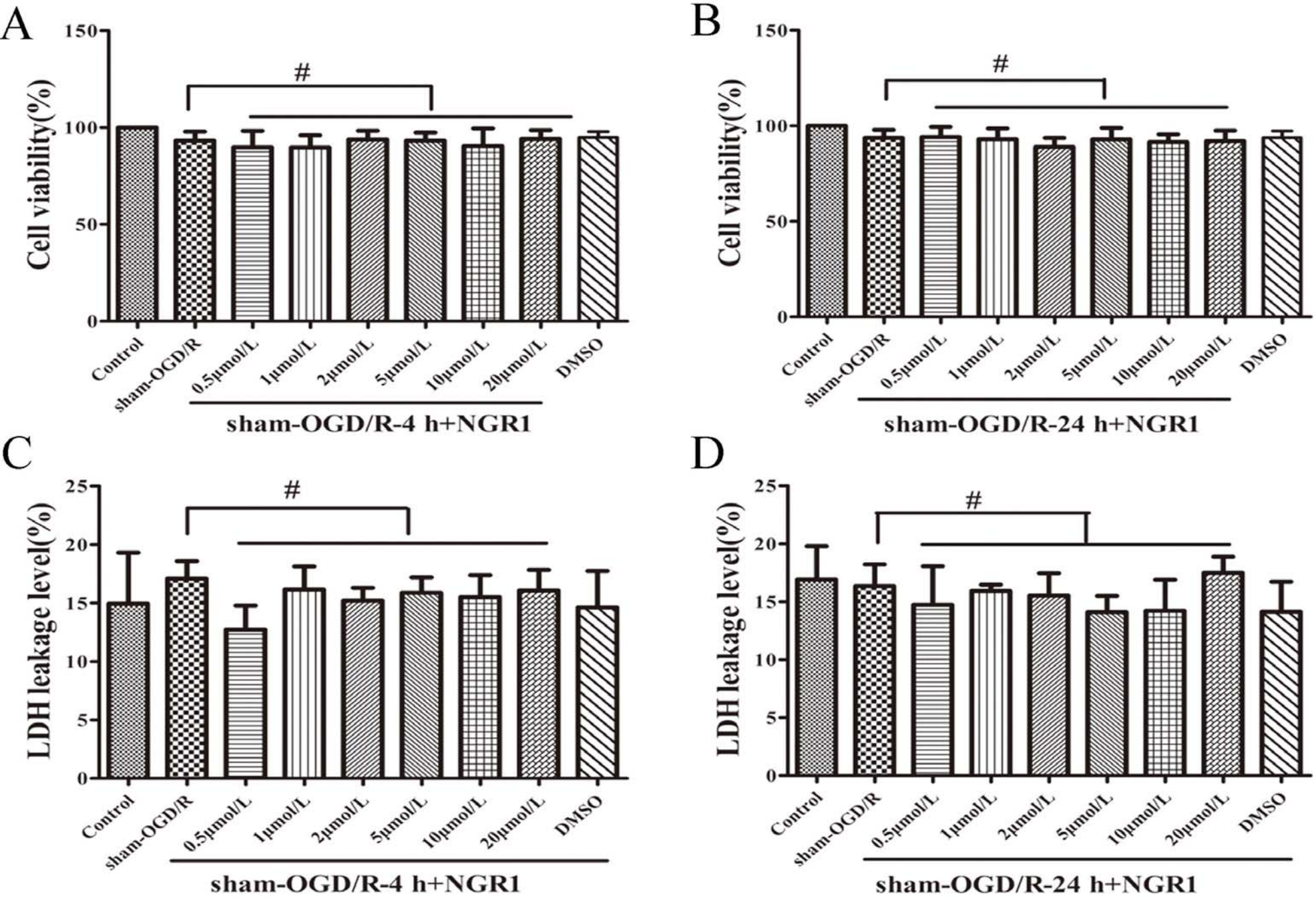

Fig.2

JPET Fast Forward. Published on February 18, 2016 as DOI: 10.1124/jpet.115.230359
This article has not been copyedited and formatted. The final version may differ from this version.

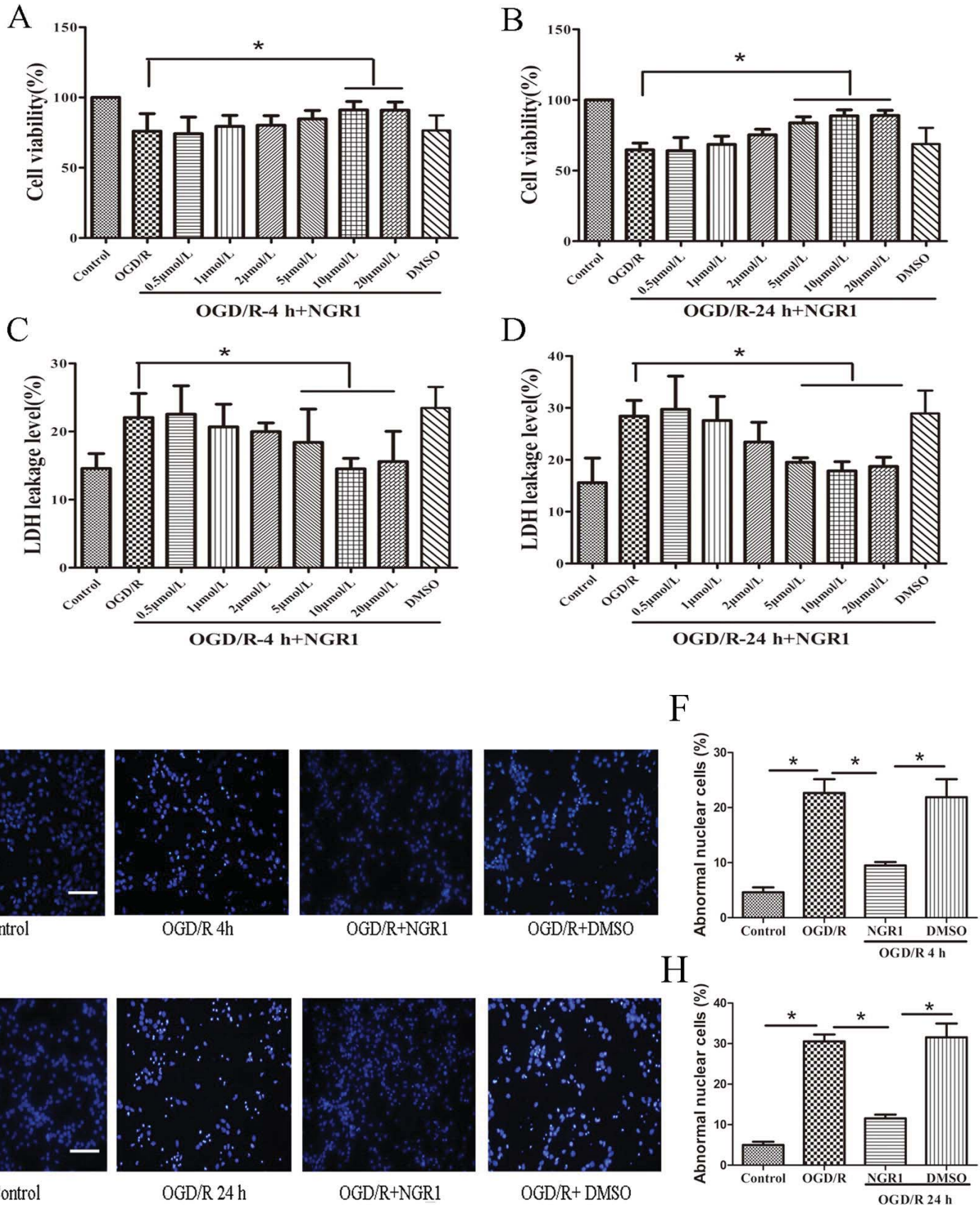

Fig.3

JPET Fast Forward. Published on February 18, 2016 as DOI: 10.1124/jpet.115.230359
This article has not been copyedited and formatted. The final version may differ from this version.

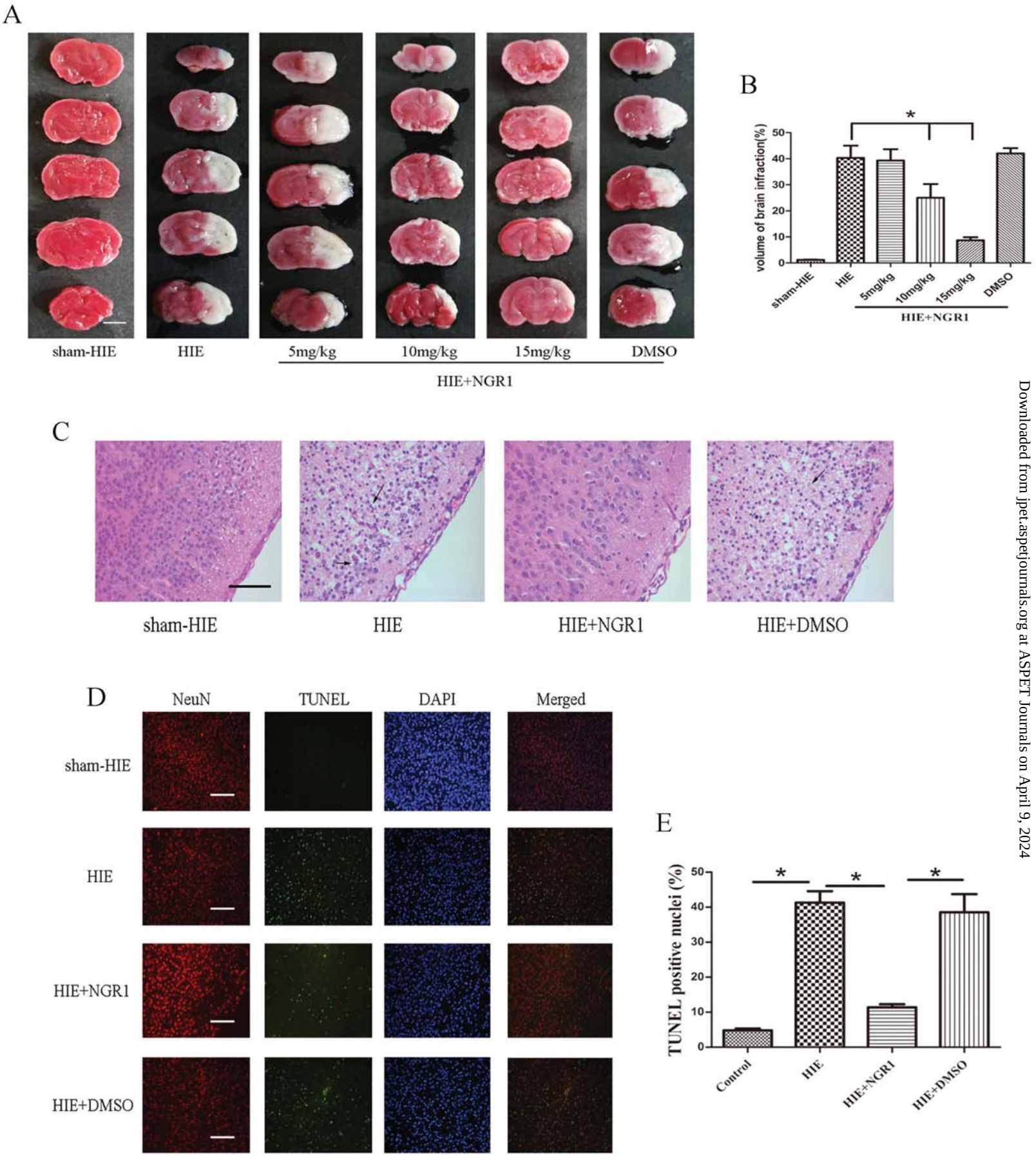

Fig.4

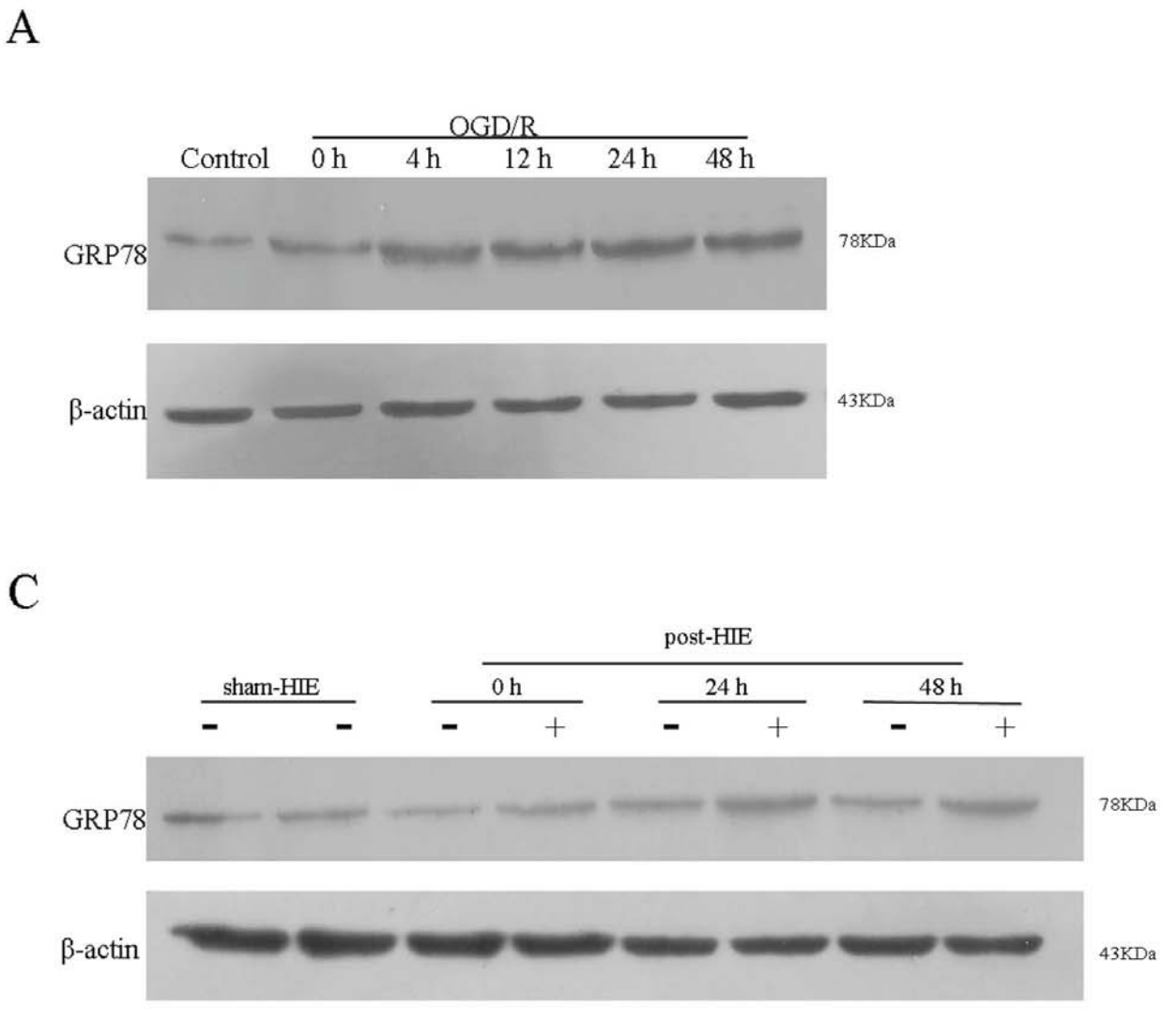

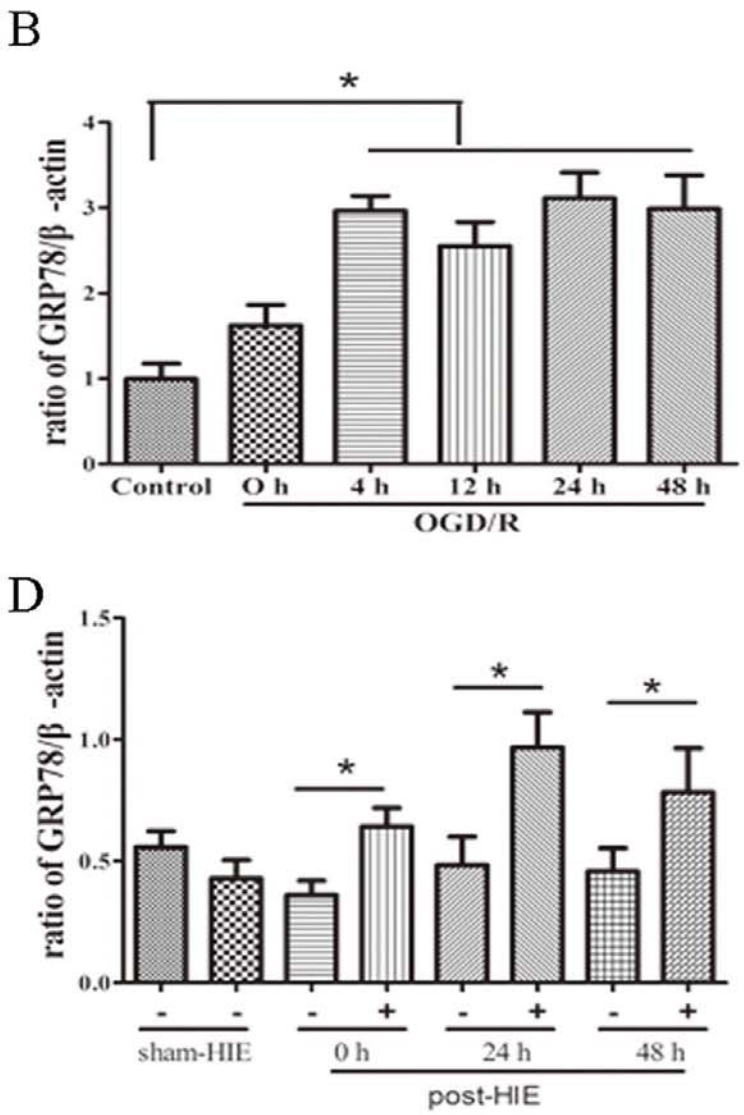

Fig.5

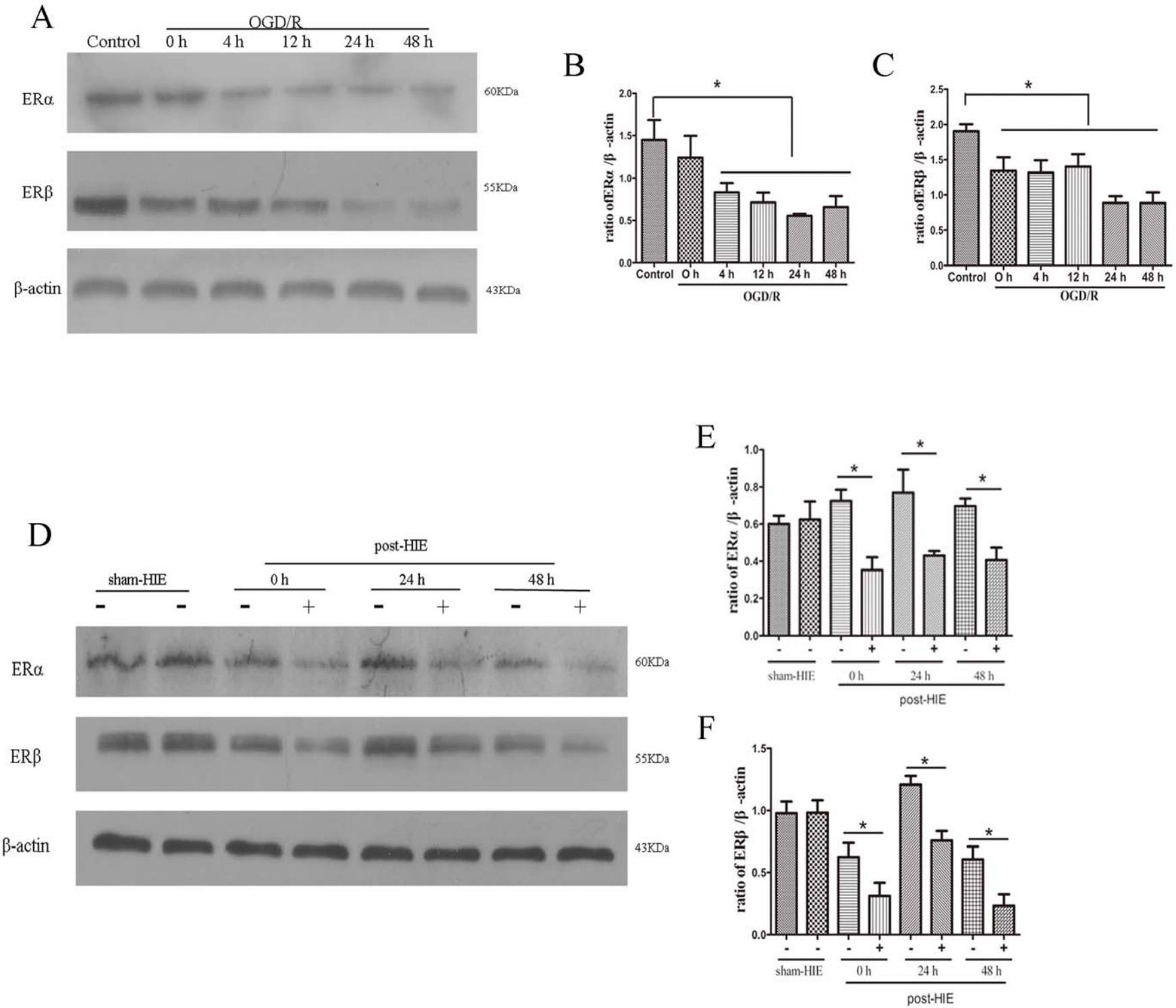

Fig.6

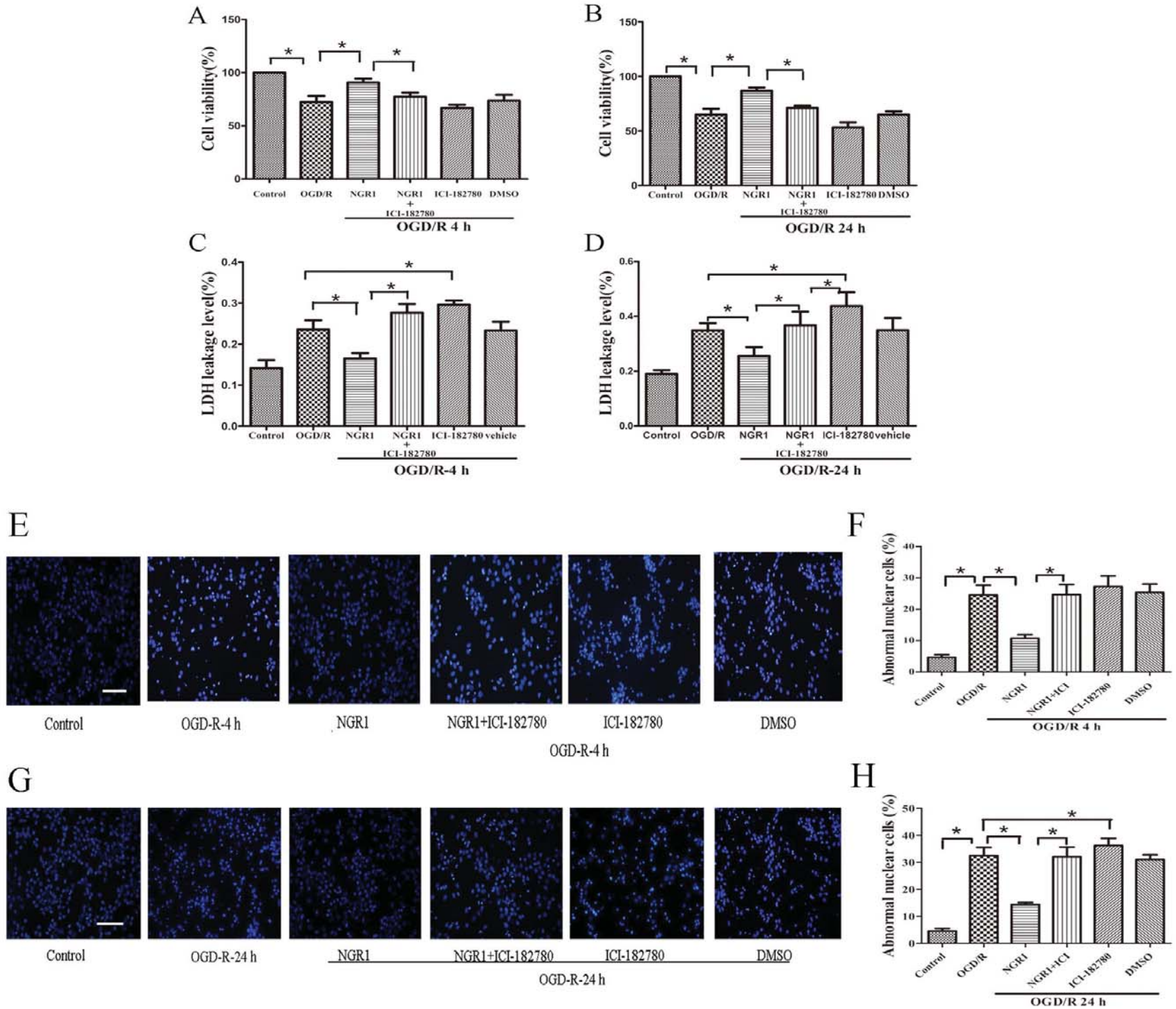

Fig.7

JPET Fast Forward. Published on February 18, 2016 as DOI: 10.1124/jpet.115.230359
This article has not been copyedited and formatted. The final version may differ from this version.

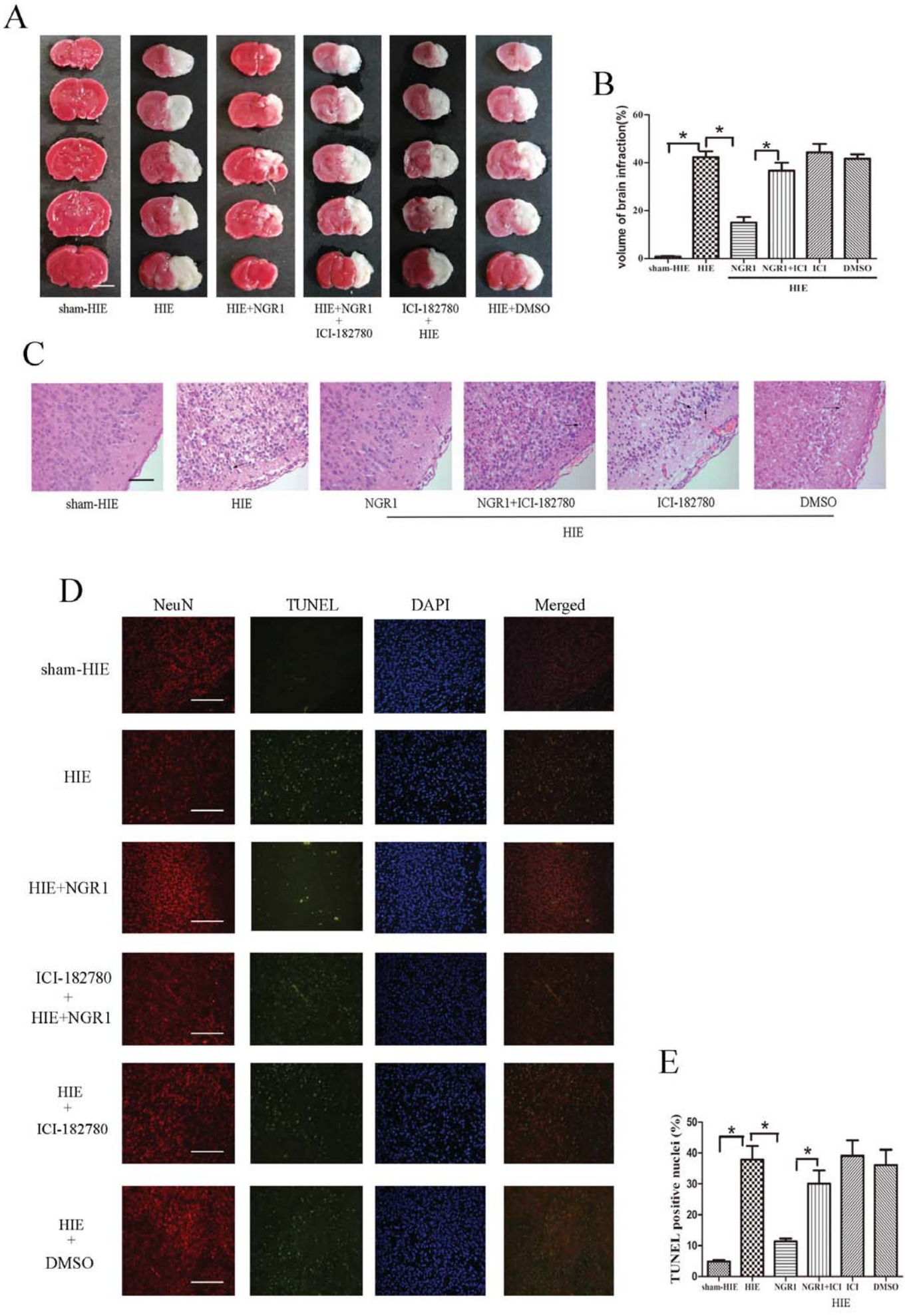

Fig.8

JPET Fast Forward. Published on February 18, 2016 as DOI: 10.1124/jpet.115.230359
This article has not been copyedited and formatted. The final version may differ from this version.

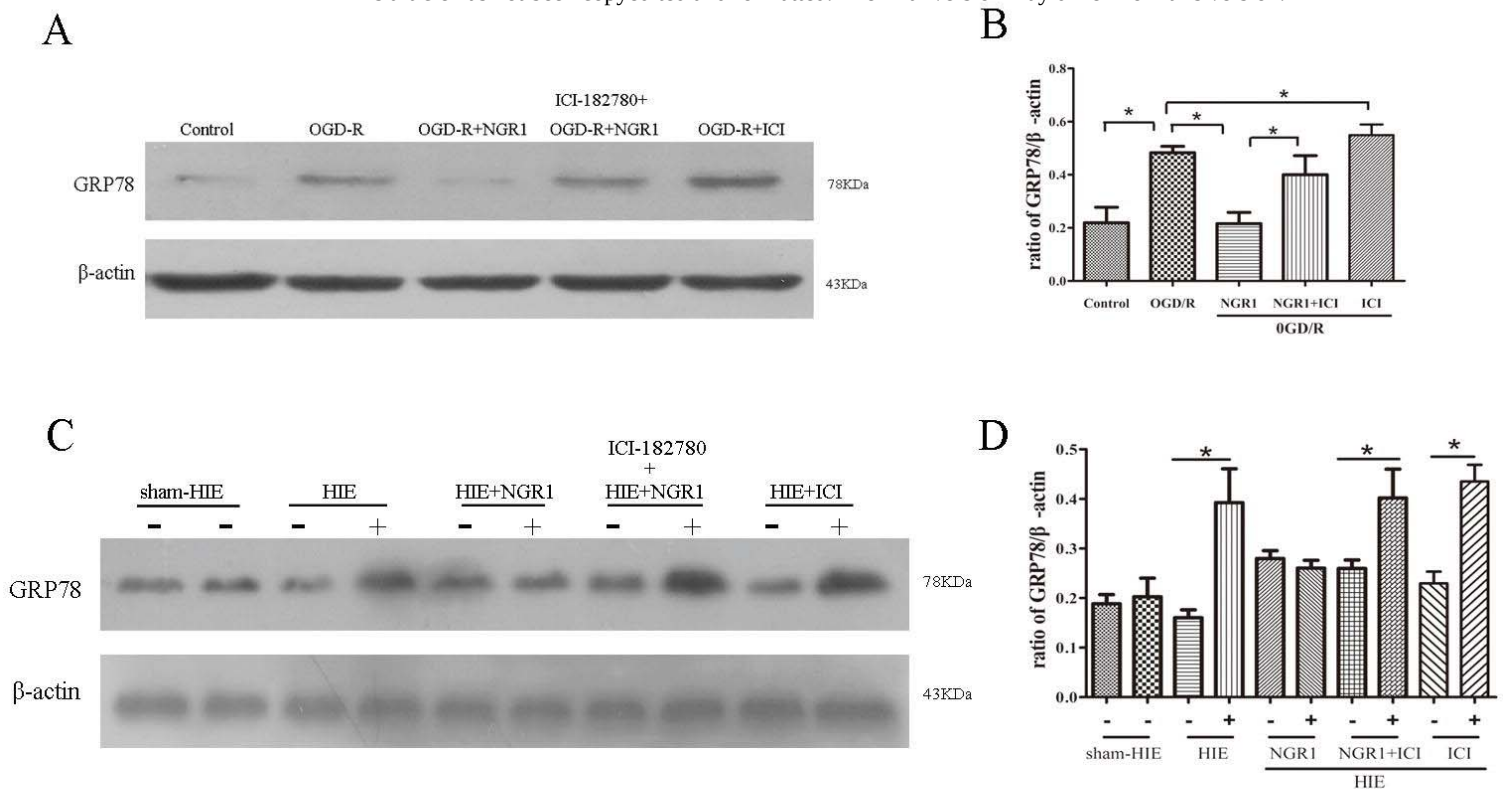

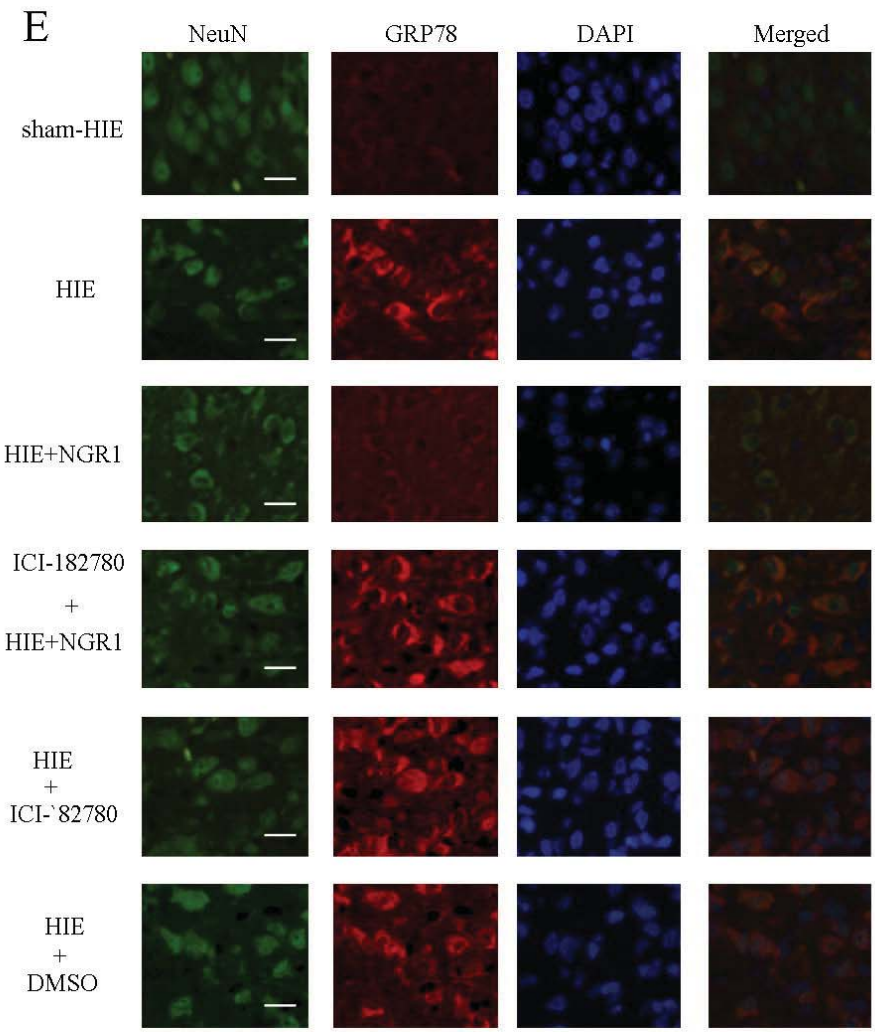

Fig.9

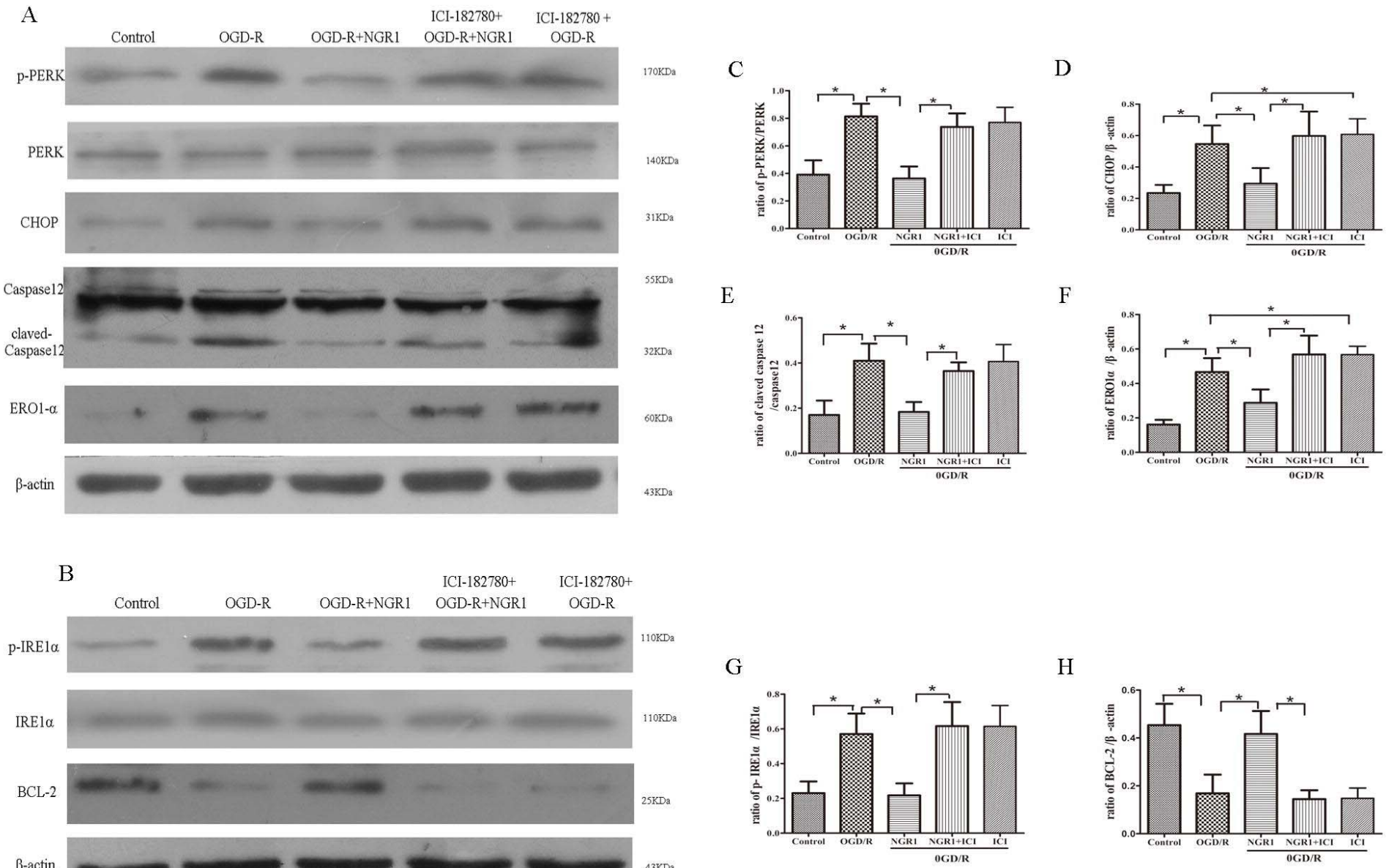

Fig.10

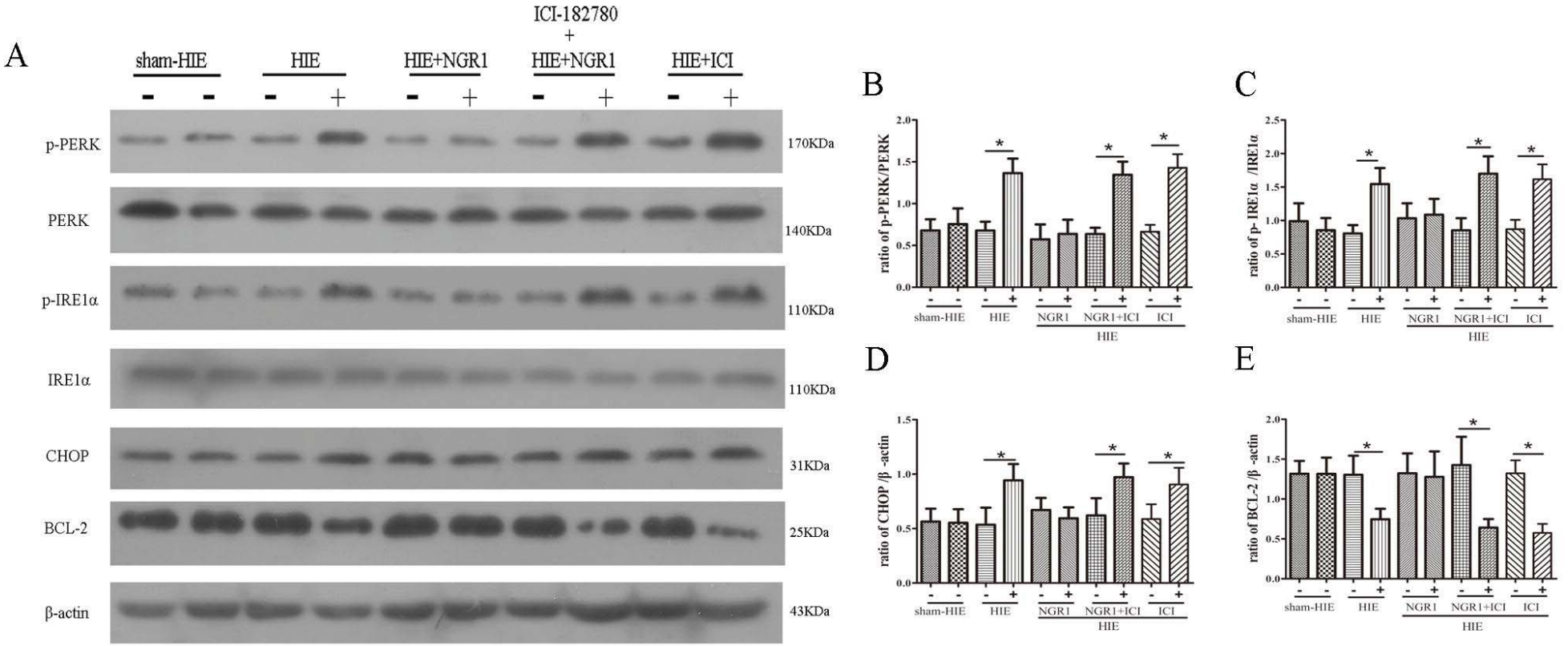

Fig.11

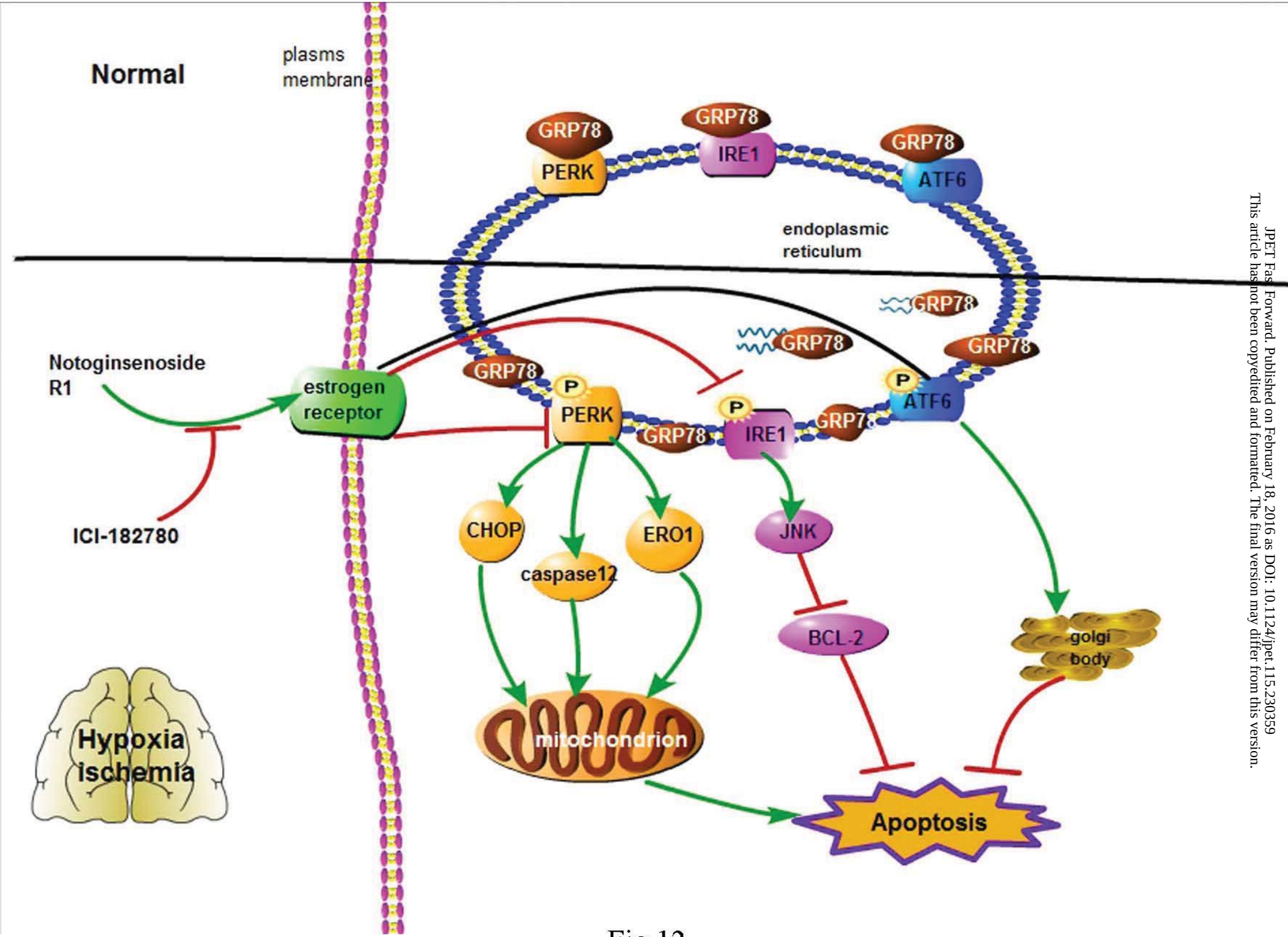

Fig.12